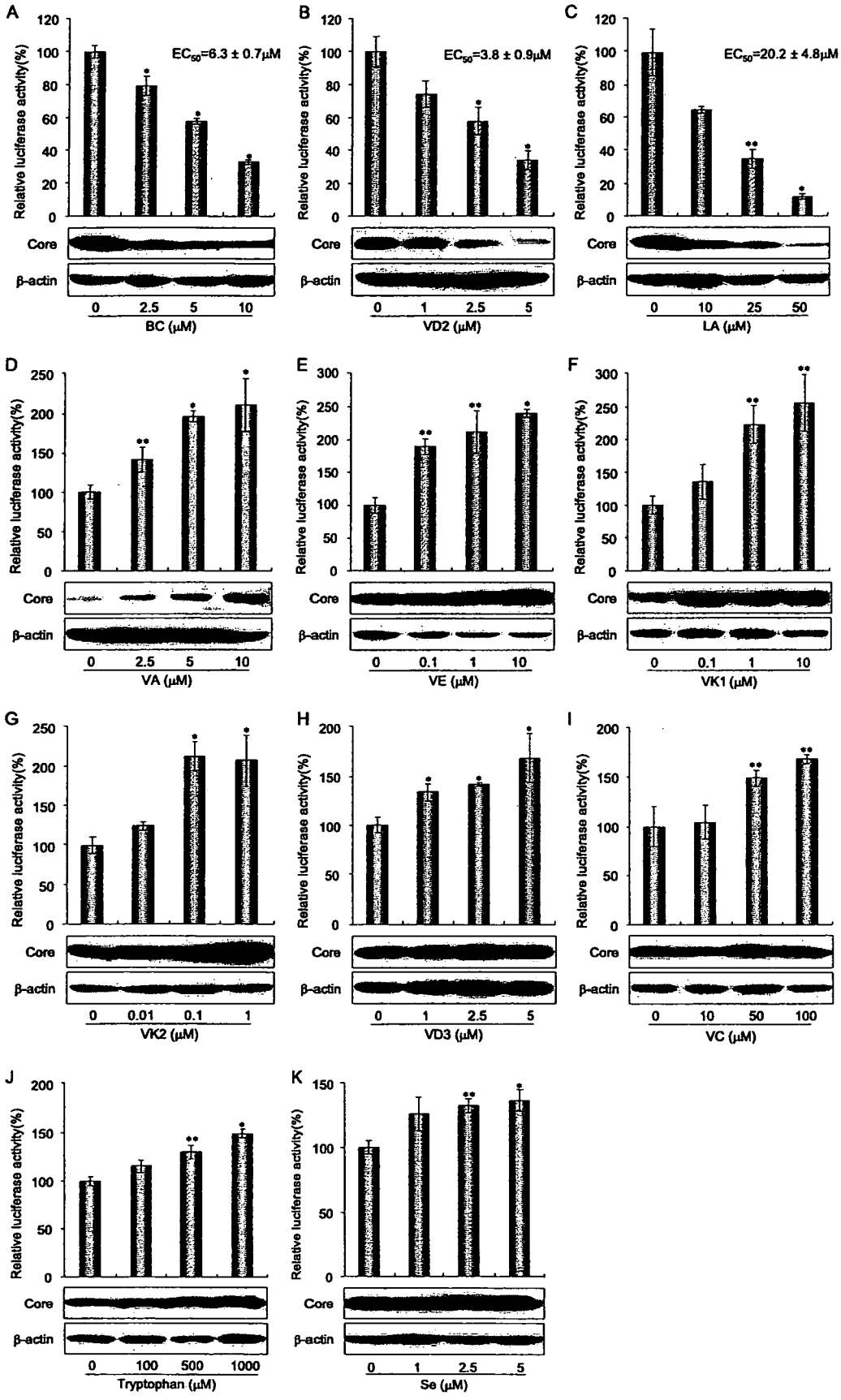

genome-length HCV RNA was eliminated by IFN-α treatment (500 IU/ml for 2 weeks) without G418, as previously described (13).

Luciferase reporter assay. For the *Renilla* luciferase (RL) assay, approximately 1.0×10^4 to 1.5×10^4 OR6 cells (72-hour treatment) or 0.5×10^4 OR6 cells (120-hour treatment) were plated onto 24-well plates in triplicate and cultured for 24 h. The cells were treated with each nutrient or compound for 72 or 120 h. Then, the cells were harvested with *Renilla* lysis reagent (Promega, Madison, WI) and subjected to the RL assay according to the manufacturer's protocol.

Western blot analysis. For Western blot analysis, 4×10^4 to 4.5×10^4 OR6c cells harboring HCV-O/KE/EG (strain O of genotype 1b) (K. Abe, M. Ikeda, and N. Kato, unpublished data) were plated onto six-well plates and cultured for 24 h and then were treated with each nutrient or compound for 72 h. Preparation of the cell lysates, sodium dodecyl sulfate-polyacrylamide gel electrophoresis, and immunoblotting were then performed as previously described (18). The antibodies used in this study were those specific to HCV core antigen (CP11; Institute of Immunology, Tokyo) and β-actin (Sigma). The epitope of CP11 was located within amino acid positions 21 to 40 of the core antigen. Immunocomplexes on the membranes were detected by enhanced chemiluminescence assay (Renaissance; Perkin Elmer Life Science, Wellesley, MA).

Cell viability. To examine the suppressive effects of nutrients on OR6 cell viability, approximately 4.5×10^4 to 5×10^4 OR6 cells (72-hour viability assay) or approximately 1×10^4 to 1.5×10^4 cells (120-hour viability assay) were plated onto six-well plates in triplicate and were cultured for 24 h. The cells were treated without nutrients or with each nutrient for 72 or 120 h, and then the number of viable cells was counted after trypan blue dye treatment as previously described (30).

Statistical analysis and synergistic statistics. Differences between the anti-HCV activities of the nutrients at each concentration and controls were tested using Student's *t* test. *P* values of less than 0.05 were considered statistically significant. Then, an isobologram method was used to evaluate the effects of a combination of nutrients or compounds on HCV RNA replication (21). OR6 cells were treated with each combination of nutrients or compounds at various concentrations for 72 h. The 50% effective concentration (EC_{50}) against HCV RNA replication in each combination treatment was analyzed by sigmoid regression, and isoboles of EC_{50} were plotted using the resulting data.

RESULTS

Effects of ordinary nutrients on HCV RNA replication. To date, information about the anti-HCV effects of ordinary nutrients has been limited to only a few studies, and in those studies, a plasmid (26), a subgenomic replicon (21), and recombinant HCV proteins (5, 8, 9) were used in the assays. We recently developed OR6 assay system by the selection after introducing genome-length ORN/C-5B/KE RNA (Fig. 1A) into HuH-7 cells. Our OR6 assay system renders it possible to carry out the prompt and precise evaluation of genome-length HCV RNA replication (13, 30). Therefore, we comprehensively analyzed 46 ordinary nutrients to determine their effects on HCV RNA replication using our novel OR6 assay system (Table 1). The effects of the preexistent nutrients in the medium on HCV RNA replication were under a significant level, because the concentrations of the nutrients already contained in the medium were less than a one-thousandth part of the minimum concentration in the treatment.

We first examined 8 liposoluble vitamins and 10 water-soluble vitamins to investigate their effects on HCV RNA replication. Among the liposoluble vitamins, VA (Fig. 2D), VE (Fig. 2E), and VK (Fig. 2F and G) significantly enhanced HCV RNA replication. However, BC and VD2 significantly inhibited HCV RNA replication in a dose-dependent manner (the mean EC_{50}s ± standard deviations [SDs] were 6.3 ± 0.7 μM and 3.8 ± 0.9 μM, respectively) (Fig. 2A and B). In contrast with VD2, VD3 apparently enhanced relative luciferase activity, but this promotive effect was thought to result from cell proliferation, since the amount of β-actin increased in a manner similar to that of HCV core antigen (Fig. 2H). Most of the water-soluble vitamins exerted no effect on HCV RNA replication (data not shown), while only VC moderately enhanced HCV RNA replication (Fig. 2I).

We next examined three branched-chain amino acids and three aromatic amino acids for their effects on HCV RNA replication. We tested the six amino acids at concentrations of 0, 100, 500, and 1,000 μM, and only tryptophan exerted moderate promotive effects on HCV RNA replication (Fig. 2J).

We further examined four saturated fatty acids, three monounsaturated fatty acids, and four polyunsaturated fatty acids (PUFAs) to assess their effects on HCV RNA replication. As has been noted in previous reports (17, 21), all of the PUFAs, i.e., LA, AA, EPA, and DHA, inhibited HCV RNA replication in OR6 cells in a dose-dependent manner (the mean EC_{50}s ± SDs were 20.2 ± 4.8 μM, 22.1 ± 1.7 μM, 36.2 ± 2.5 μM, and 37.0 ± 3.6 μM, respectively). However, we found that with the exception of LA, treatment with 50 μM of PUFA resulted in

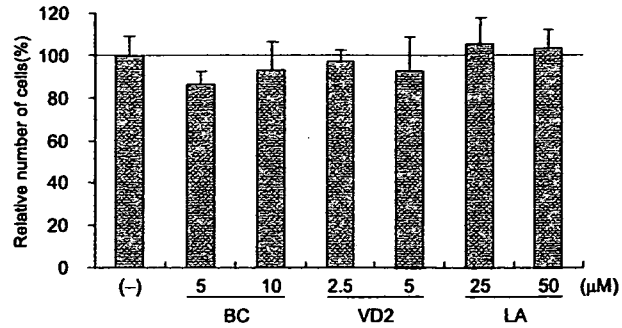

FIG. 3. The anti-HCV activities of three nutrients were not due to the suppression of cell growth. Cell viabilities after treatment with BC, VD2, and LA are shown. OR6 cells were cultured in control medium [(−)] and in the presence of BC (5 and 10 μM), VD2 (2.5 and 5 μM), and LA (25 and 50 μM) for 72 h, and then the number of viable cells was counted after trypan blue dye treatment. Shown here are the percent relative cell numbers calculated when the relative cell number of untreated cells was assigned as 100%. The data indicate means ± SDs of triplicates from at least two independent experiments.

FIG. 2. Effects of ordinary nutrients on HCV RNA-replicating cells. (A through K) Reporter assay and Western blot analysis of nutrient sensitivity of HCV RNA replication. OR6 cells were treated with each nutrient at a four-grade-modulated concentration in the medium. After 72 h of treatment, the RL assay was performed as described in Materials and Methods. Shown here are the percent relative luciferase activities calculated when the RL activity of untreated cells was assigned the value of 100%. The data indicate means ± SDs of triplicate samples from at least three independent experiments. Subsequently, OR6c cells, into which authentic HCV RNA was introduced, were treated with nutrients exhibiting either inhibitory effects, i.e., BC (A), VD2 (B), and LA (C), or promotive effects, i.e., VA (D), VE (E), VK1 (F), VK2 (G), VD3 (H), VC (I), tryptophan (J), and Se (K) at the same concentrations as those used in the OR6 assay (bar graphs). After 72 h of treatment, the production of HCV core antigen was analyzed by immunoblotting using antibody specific to HCV core antigen (upper lanes). β-Actin was used as a control for the amount of protein loaded per lane (lower lanes). *, $P < 0.01$; **, $P < 0.05$.

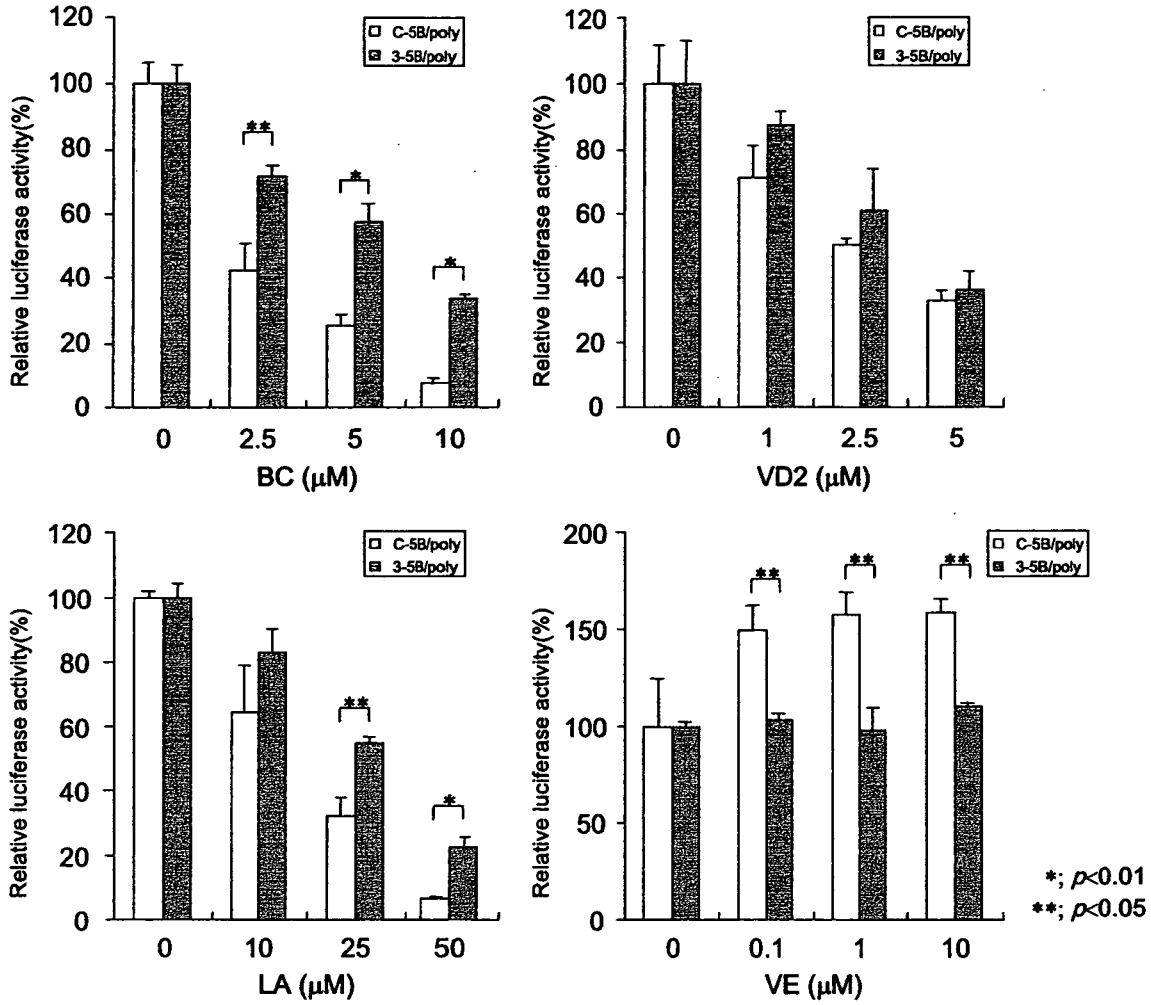

FIG. 4. The effects of BC, VD2, LA, and VE on polyclonal genome-length and subgenomic HCV RNA replication. Both polyclonal genome-length HCV RNA-replicating cells (ORN/C-5B/KE/poly) and subgenomic replicon cells (ORN/3-5B/KE/poly) were treated with BC, VD2, LA, or VE according to the same protocol as that used for the OR6 assay. The RL assay was performed at 72 h postapplication, and then RL activity was calculated as described in the legend to Fig. 2.

the suppression of cell growth due to cytotoxicity (data not shown). These data indicate that among PUFAs, only LA exhibited a significant inhibitory effect on HCV RNA replication without concomitant cytotoxicity (Fig. 2C and 3).

Finally, we examined 11 salts in order to assess their effects on HCV RNA replication. Iron [Fe(II) in the form of $FeSO_4$ and Fe(III) in the form of $Fe(NO_3)_3$] and zinc (in the form of $ZnCl_2$) exhibited anti-HCV effects without cytotoxicity at concentrations of up to 50% inhibition, but beyond 50% inhibition, cell growth was dose-dependently affected by the cytotoxicity of these minerals. Selenium (in the form of Na_2SeO_4), a typical antioxidant, slightly enhanced HCV RNA replication (Fig. 2K). We also confirmed these results using authentic HCV RNA-replicating cells (Fig. 1B and 2A through K).

These results suggest that the ordinary nutrients tested here have different profiles in terms of their effects on HCV RNA replication. The results are summarized in Table 1. Most of the nutrients were found to have no effect on HCV RNA replication. Eight nutrients enhanced HCV RNA replication, and the antioxidant nutrients VA, VC, VE, and Se were included in this group. Among the 46 nutrients tested with the OR6 assay system, we found that BC, VD2, and LA exerted anti-HCV effects without cytotoxicity. To the best of our knowledge, this is the first study to demonstrate the anti-HCV effects of BC and VD2. Therefore, we focused on the anti-HCV effects of BC, VD2, and LA in the following study.

The effects of BC, VD2, LA, and VE on polyclonal genome-length and subgenomic HCV RNA replication. OR6 cells are among the cloned cell lines selected by G418. Therefore, we examined polyclonal cells harboring genome-length HCV RNA (ORN/C-5B/KE/poly) to exclude the possibility that the anti-HCV effects of BC, VD2, and LA were an OR6 clone-specific phenomenon. Furthermore, polyclonal cells harboring subgenomic HCV RNA (ORN/3-5B/KE/poly) were also used to examine the effects of the anti-HCV nutrients on RNA replication in the absence of the structural HCV proteins. The

results revealed that all of these three nutrients exhibited a dose-dependent suppression of HCV RNA replication in both cell systems, although the three nutrients had stronger anti-HCV effects in the polyclonal genome-length HCV RNA-replicating cells than they did in the subgenomic HCV RNA-replicating cells (Fig. 4). These results indicated that the anti-HCV activities of these nutrients were not due to cell clonality, and the sensitivities of the reagents were found to differ between subgenomic and genome-length HCV RNA-replicating cells. One possible explanation of this difference is that the different genome sizes of subgenomic (9-kb) and genome-length (12-kb) HCV RNA might affect the replication efficiencies and lead to the difference in the sensitivities of antiviral reagents. These differences were significant, especially in BC- and LA-treated cells. A subgenomic replicon system may underestimate the effects of anti-HCV reagents and therefore might fail to identify potentially effective anti-HCV reagents. Therefore, our genome-length HCV RNA replication system (OR6) is advantageous for evaluating anti-HCV candidates.

We also tested VE's effect on subgenomic and genome-length HCV RNA-replicating cells. VE enhanced the replication of genome-length HCV RNA. However, interestingly, VE did not affect subgenomic HCV RNA replication. These results suggest that the subgenomic HCV RNA replication system may not be able to evaluate the reagent-enhancing HCV RNA replication.

Anti-HCV activities of three nutrients were not due to inhibition of cell growth. Since it has been reported that HCV RNA replication is dependent on cell growth (34), we examined whether the anti-HCV activities of three nutrients were due to their respective cytotoxicities. OR6 cells were treated with each nutrient (BC, 5 and 10 μM; VD2, 2.5 and 5 μM; LA, 25 and 50 μM) for 72 h. These results suggest that the anti-HCV effects of BC, VD2, and LA are not due to their cytotoxicities.

Time course assay of inhibitory effects of three nutrients on HCV RNA replication. A kinetics analysis of the anti-HCV effects of reagents provides information about inhibitory mechanisms and optimized drug administration. Therefore, we conducted a time course assay (24, 72, and 120 h after treatment) of the anti-HCV effects of three nutrients, BC, VD2, and LA, using our OR6 assay system. The results revealed that BC and VD2 exhibited stronger inhibition of HCV RNA replication than did LA at 24 h after treatment. However, the anti-HCV activities of BC and VD2 only slightly increased at 72 or 120 h after treatment (Fig. 5A). On the other hand, LA inhibited HCV RNA replication in dose- and time-dependent manners. It is noteworthy that about 90% inhibition of RL activity was observed at 120 h after LA (50 μM) treatment of OR6 cells (Fig. 5A).

We examined whether these reductions in relative RL activity induced by all three nutrients at 120 h were due to the suppression of cell growth. Compared to the number of untreated cells, at 120 h after treatment with each nutrient (BC, 5 and 10 μM; VD2, 2.5 and 5 μM; LA, 25 and 50 μM), no significant reduction in the number of treated cells was observed (Fig. 5B). These results indicate that the anti-HCV effects of these three nutrients were not due to their respective cytotoxicities.

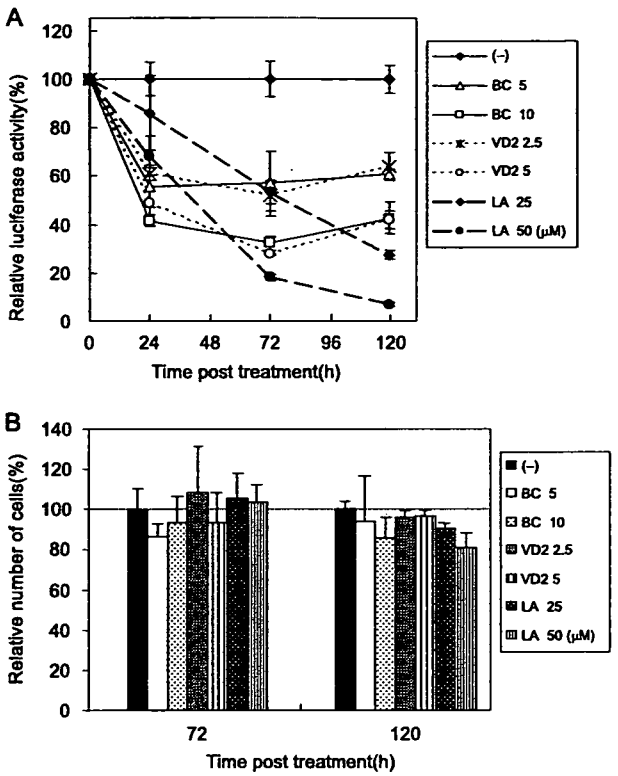

FIG. 5. Time course assay of the anti-HCV activities of three nutrients. (A) Time course of the inhibitory effects of three nutrients on HCV RNA replication. OR6 cells were treated with control medium [(−)], BC (5 and 10 μM), VD2 (2.5 and 5 μM), or LA (25 and 50 μM), and the RL assay was performed at 24, 72, and 120 h postapplication. Relative RL activity was calculated as described in the legend to Fig. 2. (B) Time course of cell viability after the application of three nutrients. OR6 cells were cultured in the control medium and in the presence of BC (5 and 10 μM), VD2 (2.5 and 5 μM), or LA (25 and 50 μM), and at 72 and 120 h postapplication, the number of viable cells was counted after trypan blue dye treatment. Shown here are the percent relative cell numbers calculated as described in the legend to Fig. 3.

HCV RNA replication was additively inhibited by each combination of three nutrients and was synergistically inhibited by all three. As described above, we found that BC, VD2, and LA possessed anti-HCV activities. However, these nutrients appeared to be insufficient for eliminating HCV by mono-treatment. Therefore, we examined the anti-HCV effects of two or three nutrients in combination.

To evaluate the effects of each combination treatment, OR6 cells were cotreated with two nutrients at the listed concentrations for 72 h (BC, approximately 0 to 5 μM; VD2, approximately 0 to 3 μM; LA, approximately 0 to 20 μM). Isoboles of 50% inhibition of HCV RNA replication were obtained for each data point. An analysis of the 50% isoboles of each combination treatment graphed nearly a straight line in each case. These results indicate that the inhibitory effects of all combinations on HCV RNA replication were additive (Fig. 6A).

Treatment with all three nutrients at various concentrations resulted in stronger suppression of HCV RNA replication in OR6 cells than we had predicted as an additive effect (Fig. 6B).

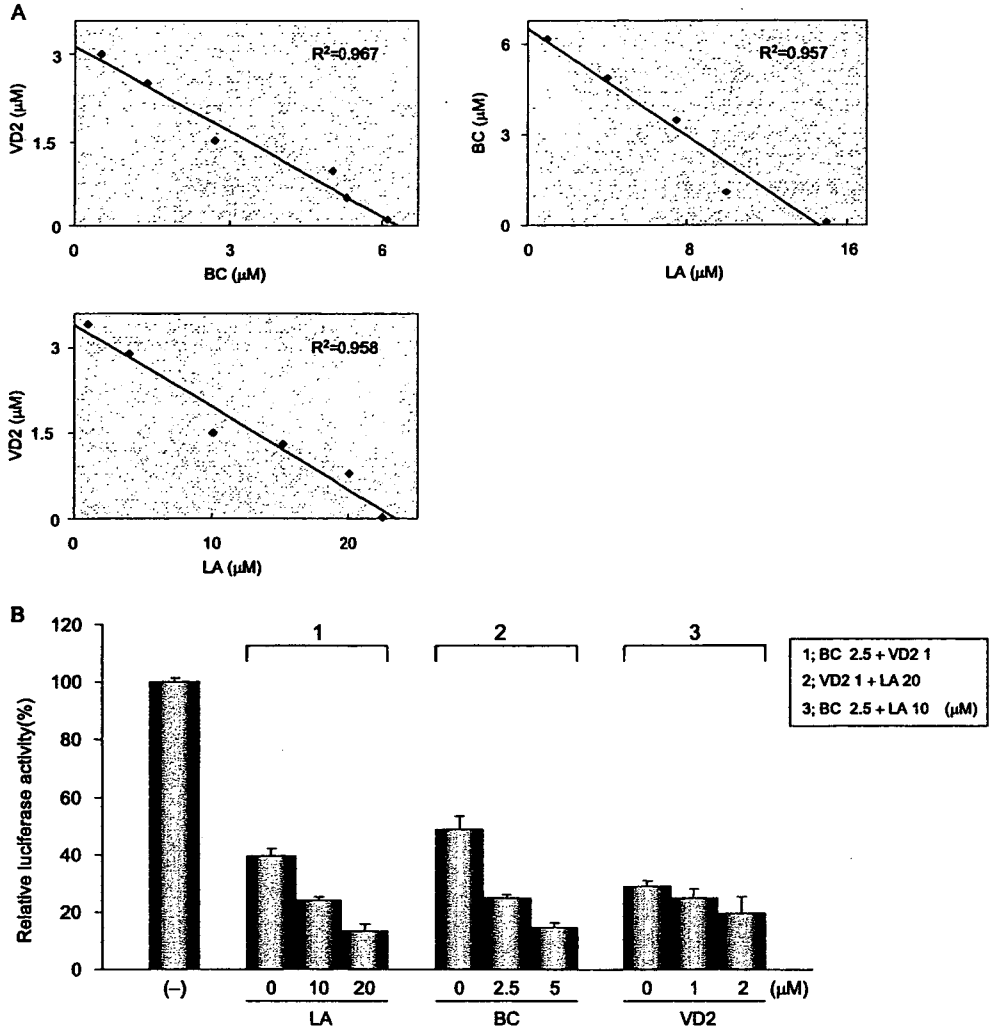

FIG. 6. Effects of treatment with each combination or all of the three nutrients on HCV RNA replication. (A) Isobole plots of 50% inhibition of HCV RNA replication. OR6 cells were treated with each combination of three nutrients, BC (0, 0.5, 1, 2, 3, 4, and 5 μM), VD2 (0, 0.1, 0.5, 1, 1.5, 2, and 3 μM), and LA (0, 1, 5, 10, 15, and 20 μM), for 72 h, and RL assay was performed as described in the legend to Fig. 2 to obtain 50% isoboles. The R^2 value indicates the coefficient of determination. (B) The effect of treatment with all three nutrients on HCV RNA replication was synergistic. OR6 cells were treated with LA (0, 10, and 20 μM) in addition to 2.5 μM BC plus 1 μM VD2, BC (0, 2.5, and 5 μM) in addition to 1 μM VD2 plus 20 μM LA, or VD2 (0, 1, and 2 μM) in addition to 2.5 μM BC plus 10 μM LA. After 72 h of treatment, the RL assay was performed, and then relative RL activity was calculated as described in the legend to Fig. 2.

For instance, in the sample cotreated with 2.5 μM BC (≈EC_{20}) in addition to 1 μM VD2 (≈EC_{30}) plus 20 μM LA (≈EC_{50}) (Fig. 2A through C), the actual effect on HCV RNA replication was 90% inhibition, which was 20% greater than we had originally estimated (i.e., approximately 70%; $1 - 0.8 \times 0.7 \times 0.5 = 0.72$) (Fig. 6B). In addition, no suppression of cell growth was observed during these cotreatments (data not shown). These results suggest that treatment with a mixture of these three nutrients may exert synergistic inhibitory effects on HCV RNA replication.

Treatment with each of three nutrients in combination with IFN or FLV additively inhibited HCV RNA replication, and CsA synergistically inhibited HCV RNA replication. Recently, CsA was proposed as a novel candidate to be paired with IFN in similar studies using a cell culture system (41). We have also reported findings obtained with 3-hydroxy-3-methylglutaryl coenzyme A reductase inhibitors, statins, exerted diverse anti-HCV effects, and FLV was found to exert the strongest inhibitory effect on HCV RNA among the statins tested (14).

Therefore, we examined the anti-HCV effects of each of three nutrients in combination with IFN, FLV, or CsA by using OR6 cells. OR6 cells were treated for 72 h with IFN-α (0, 0.2, 0.5, and 1 IU/ml) in combination with each of the nutrients at various concentrations (BC, approximately 0 to 5 μM; VD2, approximately 0 to 4 μM; LA, approximately 0 to 20 μM) (Fig. 7A). FLV (approximately 0 to 2 μM) or CsA (approximately 0 to 1 μg/ml) was also used for treatment in combination with BC, VD2, or LA at the concentration mentioned above (Fig. 7B and C). Isoboles of 50% inhibition of HCV RNA replication were generated from each sample. An analysis of 50%

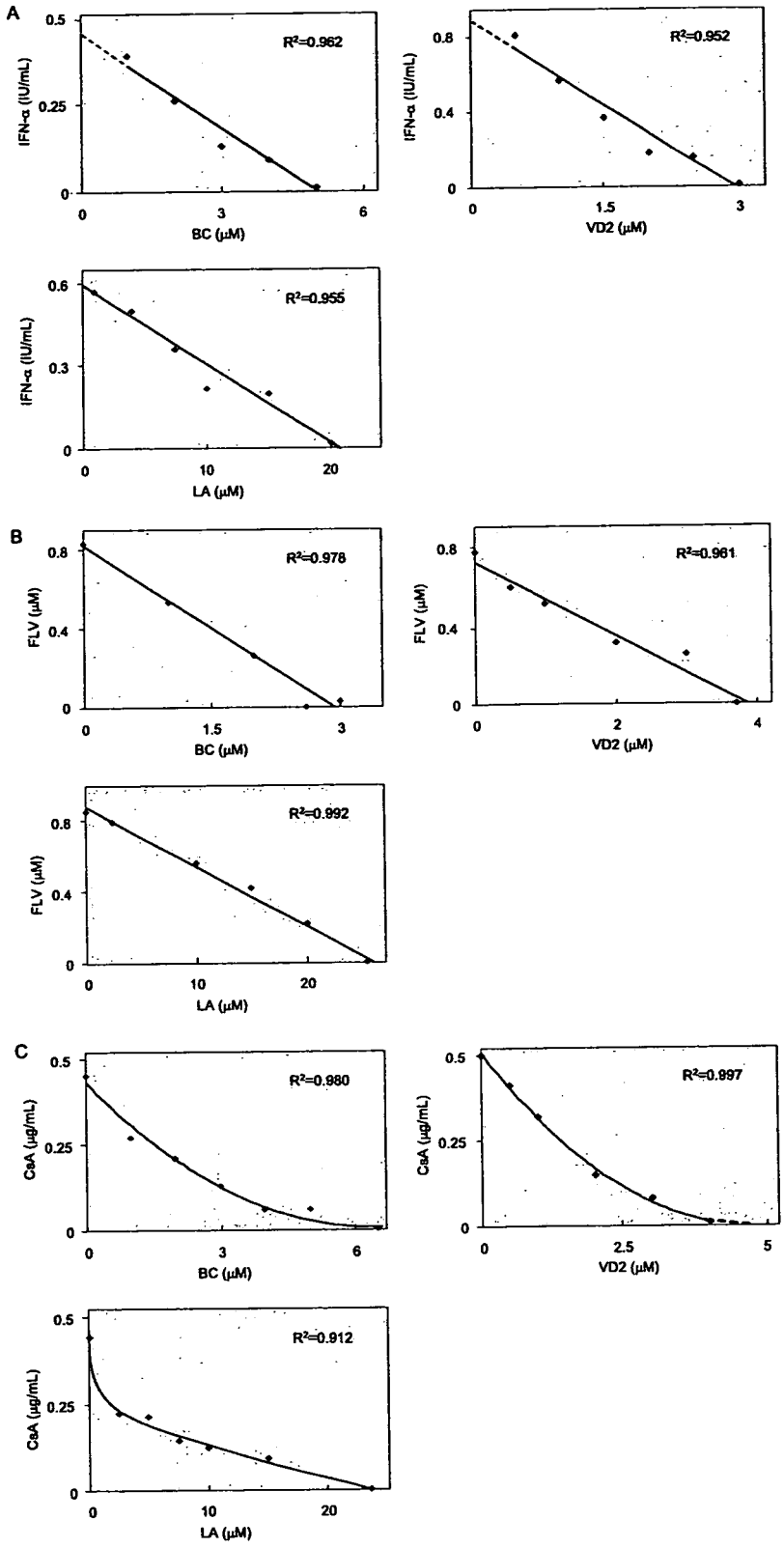

FIG. 7. Additive inhibitory effects of each of three nutrients in combination with IFN-α or FLV on HCV RNA replication, and synergistic effects observed with Cs. (A to C) Isobole plots of 50% inhibition of HCV RNA replication. OR6 cells were treated with BC (0, 1, 2, 3, 4, and 5 μM), VD2 (0, 0.5, 1, 2, 3, and 4 μM), and LA (0, 2.5, 5, 10, 15, and 20 μM) in combination with IFN-α (0, 0.2, 0.5, and 1 IU/ml) (A), FLV (0, 0.5, 1, and 2 μM) (B), or CsA (0, 0.2, 0.5, and 1 μg/ml) (C) for 72 h, and the RL assay was performed as described in the legend to Fig. 2 to obtain 50% isoboles. The R^2 value indicates the coefficient of determination.

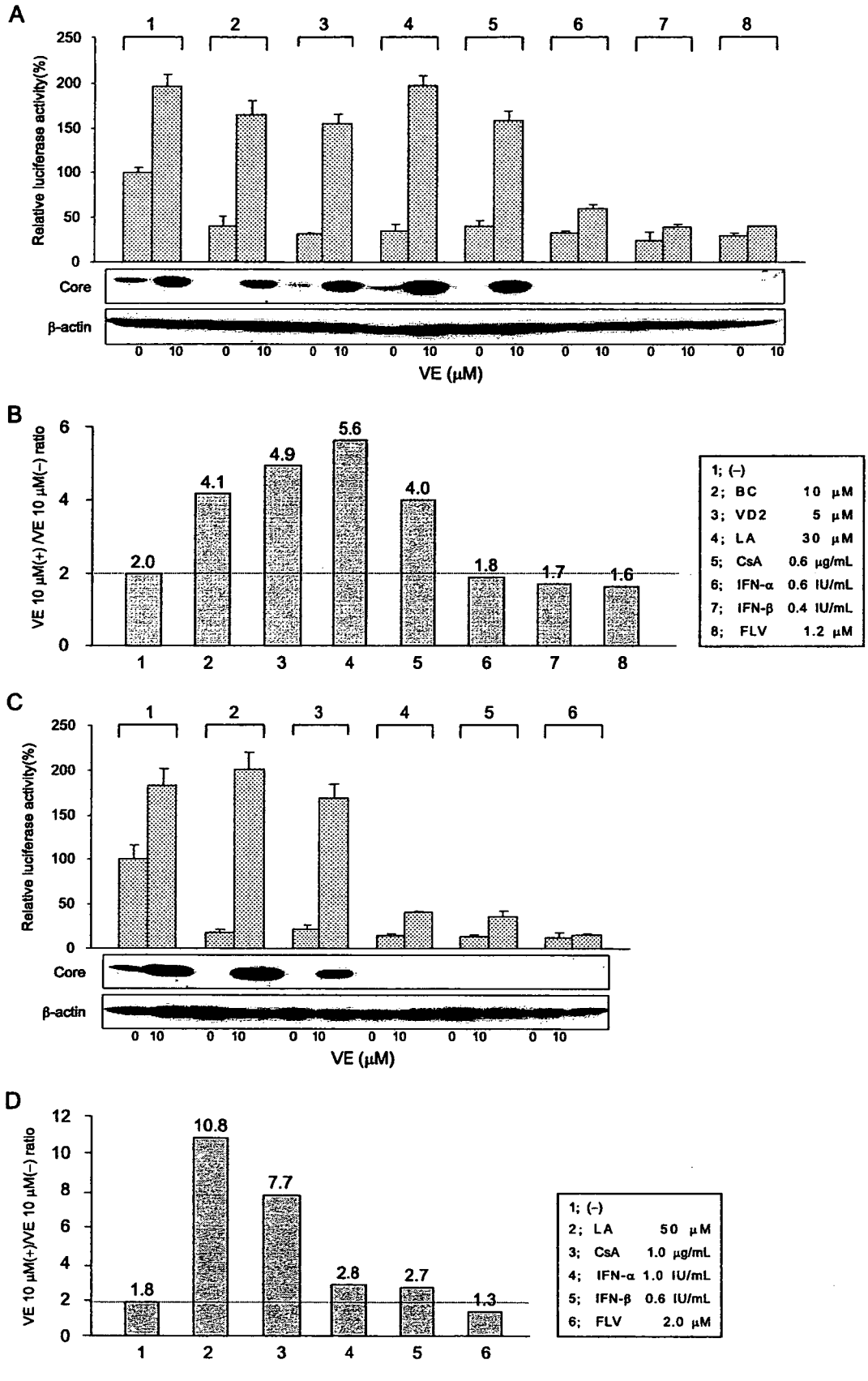

isoboles in combinations using each nutrient and IFN-α or FLV graphed nearly straight lines in each case, indicating that the suppressive effects of these cotreatments on HCV RNA replication were additive (Fig. 7A and B). Similar additive effects were obtained in combination with IFN-β (data not shown). It was noteworthy that all cotreatments with each nutrient and CsA resulted in curved, concave plots of 50% isoboles, thus suggesting that these combinations with CsA exerted synergistic inhibitory effects on HCV RNA replication (Fig. 7C). These results indicate that these three nutrients, administered as a supportive nutritional therapy, could potentially improve the SVR rate associated with IFN therapy alone.

The anti-HCV activities of BC, VD2, and LA, as well as that of CsA but not those of IFN and FLV, were completely canceled by VE. Among the 46 nutrients tested, BC and VD2 exhibited inhibitory effects on HCV RNA replication up to 70%, and LA exhibited inhibitory effects up to 90%, without exhibiting any cytotoxicity (Fig. 5A). In contrast, most of the liposoluble vitamins enhanced HCV RNA replication in OR6 cells. We used VE in the following studies because VE is one of the most common vitamins in the daily diet and it exerts a strong enhancing effect on HCV RNA replication. To clarify the mechanism of these opposing effects, we investigated whether the anti-HCV effects of BC, VD2, and LA were canceled by the addition of VE. We also tested representative anti-HCV compounds (i.e., CsA, IFN-α, IFN-β, and FLV) in combination with VE. We first examined the influence of 10 μM VE on the nutrients and compounds at the 70% inhibitory concentration level (Fig. 8A and B). The inhibitory effects of IFN-α, IFN-β, and FLV were hardly influenced by cotreatment with VE, whereas the anti-HCV effects of BC, VD2, LA, and CsA were canceled to a significant level by VE in the OR6 cells (Fig. 8A, upper panel). These results were also confirmed using authentic HCV RNA-replicating cells (Fig. 8A, lower panel). To normalize these results, we divided the luciferase value observed in the presence of VE by that in the absence of VE, and we considered this value to represent the effects of VE. When this value was larger than the value obtained in the absence of anti-HCV reagent (2.0; column 1 in Fig. 8B), we interpreted it as indicative of a reagent whose anti-HCV effects were canceled by VE. According to this criterion, BC (4.1), VD2 (4.9), LA (5.6), and CsA (4.0) were evaluated to be reagents for which the anti-HCV effects were canceled by VE (columns 2, 3, 4, and 5 in Fig. 8B). The anti-HCV effects of IFN-α, IFN-β, and FLV were not affected by VE (columns 6, 7, and 8 in Fig. 8B). We next examined the influence of 10 μM VE on the anti-HCV nutrients and compounds at the 90% inhibitory concentration level (Fig. 8C and D). BC and VD2 were not assessed in this experiment, because the maximum inhibitory effect was 70% in the case of these nutrients (Fig. 5A). Similar results were obtained in this experiment. LA (10.8) and CsA (7.7) were evaluated to be reagents for which the anti-HCV effects were canceled by VE (compare columns 2 and 3 to column 1 in Fig. 8D), although IFN-α (2.8) and IFN-β (2.7) were slightly affected by VE at this concentration (Fig. 8D, compare columns 4 and 5 to column 1). Judging by these results, it appears that BC, VD2, LA, and CsA may share some mechanism by which VE negated their anti-HCV activities.

DISCUSSION

The differential effects of BC and VA, as well as those of VD2 and VD3, which belong to the same categories as VA and VD, respectively, are of interest. We observed that whereas BC and VD2 inhibited HCV RNA replication, VA enhanced it, and VD3 exhibited basically no effect. The mechanism governing how these vitamins from the same category exert different effects on HCV RNA remains to be elucidated. However, liposoluble vitamins have been reported to exhibit various physiological activities with each nuclear receptor, consequently acting as hormone-like substances (19, 20, 27, 35). Differences in the gene products induced by each of these vitamins may lead to differences in the effects on HCV RNA replication. Another explanation might be considered in the light of findings suggesting that VA is an antioxidant, and yet recently, BC has been reported to induce oxidative stress (32, 43). This diversity of activities among vitamins in the same category, VA, might result in a variety of influences on HCV RNA replication. Further studies are still needed to account for why these different consequences are generated.

Previous studies have demonstrated that PUFAs such as AA, EPA, and DHA inhibit HCV RNA replication in cell culture systems (17, 21). However, saturated and mono-unsaturated fatty acids have been shown to enhance HCV RNA replication (17). In the prior studies, the cells tolerated the presence of PUFAs at concentrations of up to 50 μM. In contrast, in our study, 50 μM PUFAs were toxic, with the exception of LA. Furthermore, saturated and mono-unsaturated fatty acids hardly exhibited any effects on HCV RNA replication in our OR6 cell culture system. These discrepancies might be due to differences in both the clonalities of the cells and the HCV strains used in each experiment.

FIG. 8. VE canceled the anti-HCV activities of BC, VD2, LA, and CsA. (A and B) Effects of VE on the nutrients and compounds at the 70% inhibitory concentration. Both OR6 cells and OR6c cells, into which authentic HCV RNA was introduced, were treated with control medium [(−)], 10 μM BC, 5 μM VD2, 30 μM LA, 0.6 μg/ml of CsA, 0.6 IU/ml of IFN-α, 0.4 IU/ml of IFN-β, or 1.2 μM FLV in either the absence or presence of 10 μM VE for 72 h. After treatment, an RL assay of harvested OR6 cell samples was performed, and then the relative RL activity was calculated as described in the legend to Fig. 2. Subsequently, the production of HCV core antigen in OR6c cells was analyzed by immunoblotting using antibody specific to HCV core antigen. β-Actin was used as a control for the amount of protein loaded per lane (A). Then, the ratio of RL activity in the presence of 10 μM VE (+) to the RL activity in the absence of VE (−) was calculated. The horizontal line indicates the promotive effect of 10 μM VE alone on HCV RNA replication as a baseline (B). (C and D) Effects of VE on the nutrients and compounds at the 90% inhibitory concentration. Both OR6 cells and OR6c cells were treated with control medium, 50 μM LA, 1 μg/ml of CsA, 1 IU/ml of IFN-α, 0.6 IU/ml of IFN-β, and 2 μM FLV in either the absence (−) or presence (+) of 10 μM VE for 72 h. After treatment, the RL assay and Western blot analysis were performed (C), and then the ratio of RL activity in the presence of 10 μM VE to the RL activity in the absence of VE was calculated in the same manner as that described above (D).

Here, we demonstrated that three nutrients, BC, VD2, and LA, exhibited anti-HCV effects in polyclonal genome-length and subgenomic HCV RNA (strain O of genotype 1b)-replicating cells. These results indicated that the inhibitory activities of at least three anti-HCV nutrients are not limited to a specific cell clone (OR6).

Moreover, IFN or FLV exhibited additive anti-HCV effects when the cells were cotreated with each of the three anti-HCV nutrients. However, CsA showed synergistic anti-HCV effects in combination with each of these three nutrients. Interestingly, these results coincided with the experiment using VE, as VE canceled the anti-HCV effects of CsA but not those of IFN or FLV. It was recently demonstrated that the anti-HCV effects of CsA are related to the inhibition of cyclophilin (31, 42). CsA is also known as an oxidant that can cause renal or vascular dysfunction, and interestingly, antioxidants, including VE, attenuate these CsA-induced side effects (16, 22). Furthermore, we confirmed that another antioxidant, Se, also weakened the anti-HCV effects of BC, VD2, and LA (data not shown). Therefore, BC, VD2, and LA may possess an anti-HCV mechanism similar to that of CsA, and oxidative stress may be involved in these anti-HCV effects to some extent. Among the nutrients tested, VA, VC, VE, and Se enhanced HCV RNA replication, and these nutrients functioned as antioxidants. In contrast, four PUFAs inhibited HCV RNA replication, and they served as oxidants (29, 44). These results are further evidence of the involvement of oxidative stress in HCV RNA replication.

CH C patients may take excessive doses of VE during the course of interferon therapy, because as an antioxidant, VE has been expected to prevent injury to hepatocytes caused by oxidative stress. However, our results suggest that the potentially negative effects of VE on therapy for CH C patients should be carefully considered. To date, the significance of the role played by ordinary nutrients in viral infections has not been well characterized and has even been underestimated. We believe that our findings will shed light on the field of viral infection from the perspective of the nutritional sciences.

It is difficult to determine the blood concentrations of the nutrients tested in this study because the administration conditions may affect the concentrations in the blood. Rühl et al. (35) reported that the concentrations of BC in human serum are between 0.34 to 0.54 μM and that the average concentration in the human liver is 4.4 μM. Hagenlocher et al. (12) reported that the concentration of LA in human serum is 0.8 to 11.9 μg/100 μl. Armas et al. (3) reported that the concentration of VD2 in human serum at 24 h after a 50,000-IU administration is about 50 nM. The concentration of the nutrient in this study is higher than that in those reports. Therefore, monotreatment of the nutrient may not eliminate HCV. However, these nutrients may boost the effect of IFN treatment in combination like ribavirin does.

It is worth trying to examine the effects of BC, VD2, and LA on the recently developed JFH1 infectious virus production system in a future study. Here, it remains unclear whether these three nutrients affect the production of the virus. Furthermore, the comparison of the effects of these three nutrients between HCV genotypes 1 and 2 will provide useful information for the HCV therapy, as HCV genotypes 1 and 2 respond differentially to IFN treatment.

The precise mechanism underlying the anti-HCV activities of the nutrients has not been clarified in this study. The nutrients may inhibit viral RNAs and proteins, including the internal ribosome entry site, NS3-4A serine protease, and NS5B polymerase. Further in vitro study will be needed to clarify the targets of the nutrients responsible for their anti-HCV activities. Another possibility is that the nutrients inhibit the cellular proteins required for HCV RNA replication. We are now planning a study to clarify the mechanism underlying the nutrients' anti-HCV activities.

In conclusion, we found that three nutrients, BC, VD2, and LA, inhibited HCV RNA replication in a cell culture system and that Se, tryptophan, and various vitamins (A, C, E, and K) enhanced HCV RNA replication. The anti-HCV effects of BC, VD2, and LA were reversed by VE. These results are expected to provide useful information for the improvement of the SVR rates of patients receiving the currently standard IFN therapy. In addition, these findings may contribute to the development of a nutritional supplement specific to the treatment of people with CH C.

ACKNOWLEDGMENTS

We thank Atsumi Morishita for her technical assistance and Yasuo Ariumi for his helpful discussions.

This work was supported by a Grant-in-Aid for the Third-Term Comprehensive 10-Year Strategy for Cancer Control and by a Grant-in-Aid for research on hepatitis, both from the Ministry of Health, Labor, and Welfare of Japan. K.A. was supported by a Research Fellowship from the Japan Society for the Promotion of Science for Young Scientists.

REFERENCES

1. **Alter, H. J., R. H. Purcell, J. W. Shih, J. C. Melpolder, M. Houghton, Q. L. Choo, and G. Kuo.** 1989. Detection of antibody to hepatitis C virus in prospectively followed transfusion recipients with acute and chronic non-A, non-B hepatitis. N. Engl. J. Med. **321**:1494–1500.
2. **Appel, N., T. Schaller, F. Penin, and R. Bartenschlager.** 2006. From structure to function: new insights into hepatitis C virus RNA replication. J. Biol. Chem. **281**:9833–9836.
3. **Armas, L. A., B. W. Hollis, and R. P. Heaney.** 2004. Vitamin D2 is much less effective than vitamin D3 in humans. J. Clin. Endocrinol. Metab. **89**:5387–5391.
4. **Blight, K. J., J. A. McKeating, and C. M. Rice.** 2002. Highly permissive cell lines for subgenomic and genomic hepatitis C virus RNA replication. J. Virol. **76**:13001–13014.
5. **Bougie, I., S. Charpentier, and M. Bisaillon.** 2003. Characterization of the metal ion binding properties of the hepatitis C virus RNA polymerase. J. Biol. Chem. **278**:3868–3875.
6. **Cousin, S. P., S. R. Hugl, C. E. Wrede, H. Kajio, M. G. Myers, Jr., and C. J. Rhodes.** 2001. Free fatty acid-induced inhibition of glucose and insulin-like growth factor I-induced deoxyribonucleic acid synthesis in the pancreatic beta-cell line INS-1. Endocrinology **142**:229–240.
7. **Ferencz, S., and R. Batey.** 2003. Intracerebral haemorrhage and hepatitis C treatment. J. Viral Hepat. **10**:401–403.
8. **Ferrari, E., J. Wright-Minogue, J. W. Fang, B. M. Baroudy, J. Y. Lau, and Z. Hong.** 1999. Characterization of soluble hepatitis C virus RNA-dependent RNA polymerase expressed in *Escherichia coli*. J. Virol. **73**:1649–1654.
9. **Fillebeen, C., A. M. Rivas-Estilla, M. Bisaillon, P. Ponka, M. Muckenthaler, M. W. Hentze, A. E. Koromilas, and K. Pantopoulos.** 2005. Iron inactivates the RNA polymerase NS5B and suppresses subgenomic replication of hepatitis C virus. J. Biol. Chem. **280**:9049–9057.
10. **Fried, M. W.** 2002. Side effects of therapy of hepatitis C and their management. Hepatology **36**:S237–S44.
11. **Hadziyannis, S. J., H. Sette, Jr., T. R. Morgan, V. Balan, M. Diago, P. Marcellin, G. Ramadori, H. Bodenheimer, Jr., D. Bernstein, M. Rizzetto, S. Zeuzem, P. J. Pockros, A. Lin, and A. M. Ackrill.** 2004. Peginterferon-alpha2a and ribavirin combination therapy in chronic hepatitis C: a randomized study of treatment duration and ribavirin dose. Ann. Intern. Med. **140**:346–355.
12. **Hagenlocher, T., J. Nair, N. Becker, A. Korfmann, and H. Bartsch.** 2001. Influence of dietary fatty acid, vegetable, and vitamin intake on etheno-DNA adducts in white blood cells of healthy female volunteers: a pilot study. Cancer Epidemiol. Biomarkers Prev. **10**:1187–1191.

13. Ikeda, M., K. Abe, H. Dansako, T. Nakamura, K. Naka, and N. Kato. 2005. Efficient replication of a full-length hepatitis C virus genome, strain O, in cell culture, and development of a luciferase reporter system. Biochem. Biophys. Res. Commun. 329:1350–1359.
14. Ikeda, M., K. Abe, M. Yamada, H. Dansako, K. Naka, and N. Kato. 2006. Different anti-HCV profiles of statins and their potential for combination therapy with interferon. Hepatology 44:117–125.
15. Ikeda, M., M. Yi, K. Li, and S. M. Lemon. 2002. Selectable subgenomic and genome-length dicistronic RNAs derived from an infectious molecular clone of the HCV-N strain of hepatitis C virus replicate efficiently in cultured Huh7 cells. J. Virol. 76:2997–3006.
16. Jenkins, J. K., H. Huang, K. Ndebele, and A. K. Salahudeen. 2001. Vitamin E inhibits renal mRNA expression of COX II, HO I, TGFbeta, and osteopontin in the rat model of cyclosporine nephrotoxicity. Transplantation 71:331–334.
17. Kapadia, S. B., and F. V. Chisari. 2005. Hepatitis C virus RNA replication is regulated by host geranylgeranylation and fatty acids. Proc. Natl. Acad. Sci. USA 102:2561–2566.
18. Kato, N., K. Sugiyama, K. Namba, H. Dansako, T. Nakamura, M. Takami, K. Naka, A. Nozaki, and K. Shimotohno. 2003. Establishment of a hepatitis C virus subgenomic replicon derived from human hepatocytes infected in vitro. Biochem. Biophys. Res. Commun. 306:756–766.
19. Kliewer, S. A., J. M. Lehmann, and T. M. Willson. 1999. Orphan nuclear receptors: shifting endocrinology into reverse. Science 284:757–760.
20. Landes, N., P. Pfluger, D. Kluth, M. Birringer, R. Ruhl, G. F. Bol, H. Glatt, and R. Brigelius-Flohe. 2003. Vitamin E activates gene expression via the pregnane X receptor. Biochem. Pharmacol. 65:269–273.
21. Leu, G. Z., T. Y. Lin, and J. T. Hsu. 2004. Anti-HCV activities of selective polyunsaturated fatty acids. Biochem. Biophys. Res. Commun. 318:275–280.
22. Lexis, L. A., A. Fenning, L. Brown, R. G. Fassett, and J. S. Coombes. 2006. Antioxidant supplementation enhances erythrocyte antioxidant status and attenuates cyclosporine-induced vascular dysfunction. Am. J. Transplant. 6:41–49.
23. Liang, T. J., L. J. Jeffers, K. R. Reddy, M. De Medina, I. T. Parker, H. Cheinquer, V. Idrovo, A. Rabassa, and E. R. Schiff. 1993. Viral pathogenesis of hepatocellular carcinoma in the United States. Hepatology 18:1326–1333.
24. Lindenbach, B. D., M. J. Evans, A. J. Syder, B. Wolk, T. L. Tellinghuisen, C. C. Liu, T. Maruyama, R. O. Hynes, D. R. Burton, J. A. McKeating, and C. M. Rice. 2005. Complete replication of hepatitis C virus in cell culture. Science 309:623–626.
25. Lohmann, V., F. Korner, J. Koch, U. Herian, L. Theilmann, and R. Bartenschlager. 1999. Replication of subgenomic hepatitis C virus RNAs in a hepatoma cell line. Science 285:110–113.
26. Lott, W. B., S. S. Takyar, J. Tuppen, D. H. Crawford, M. Harrison, T. P. Sloots, and E. J. Gowans. 2001. Vitamin B12 and hepatitis C: molecular biology and human pathology. Proc. Natl. Acad. Sci. USA 98:4916–4921.
27. McDonnell, D. P., D. J. Mangelsdorf, J. W. Pike, M. R. Haussler, and B. W. O'Malley. 1987. Molecular cloning of complementary DNA encoding the avian receptor for vitamin D. Science 235:1214–1217.
28. McHutchison, J. G., and M. W. Fried. 2003. Current therapy for hepatitis C: pegylated interferon and ribavirin. Clin. Liver Dis. 7:149–161.
29. Miyamoto, S., G. R. Martinez, D. Rettori, O. Augusto, M. H. Medeiros, and P. Di Mascio. 2006. Linoleic acid hydroperoxide reacts with hypochlorous acid, generating peroxyl radical intermediates and singlet molecular oxygen. Proc. Natl. Acad. Sci. USA 103:293–298.
30. Naka, K., M. Ikeda, K. Abe, H. Dansako, and N. Kato. 2005. Mizoribine inhibits hepatitis C virus RNA replication: effect of combination with interferon-alpha. Biochem. Biophys. Res. Commun. 330:871–879.
31. Nakagawa, M., N. Sakamoto, Y. Tanabe, T. Koyama, Y. Itsui, Y. Takeda, C. H. Chen, S. Kakinuma, S. Oooka, S. Maekawa, N. Enomoto, and M. Watanabe. 2005. Suppression of hepatitis C virus replication by cyclosporin a is mediated by blockade of cyclophilins. Gastroenterology 129:1031–1041.
32. Paolini, M., A. Antelli, L. Pozzetti, D. Spetlova, P. Perocco, L. Valgimigli, G. F. Pedulli, and G. Cantelli-Forti. 2001. Induction of cytochrome P450 enzymes and over-generation of oxygen radicals in beta-carotene supplemented rats. Carcinogenesis 22:1483–1495.
33. Pietschmann, T., V. Lohmann, A. Kaul, N. Krieger, G. Rinck, G. Rutter, D. Strand, and R. Bartenschlager. 2002. Persistent and transient replication of full-length hepatitis C virus genomes in cell culture. J. Virol. 76:4008–4021.
34. Pietschmann, T., V. Lohmann, G. Rutter, K. Kurpanek, and R. Bartenschlager. 2001. Characterization of cell lines carrying self-replicating hepatitis C virus RNAs. J. Virol. 75:1252–1264.
35. Rühl, R., R. Sczech, N. Landes, P. Pfluger, D. Kluth, and F. J. Schweigert. 2004. Carotenoids and their metabolites are naturally occurring activators of gene expression via the pregnane X receptor. Eur. J. Nutr. 43:336–343.
36. Sagoe-Moses, C., R. D. Pearson, J. Perry, and J. Jagger. 2001. Risks to health care workers in developing countries. N. Engl. J. Med. 345:538–541.
37. Sánchez-Tapias, J. M., M. Diago, P. Escartin, J. Enriquez, M. Romero-Gomez, R. Barcena, J. Crespo, R. Andrade, E. Martinez-Bauer, R. Perez, M. Testillano, R. Planas, R. Sola, M. Garcia-Bengoechea, J. Garcia-Samaniego, M. Munoz-Sanchez, and R. Moreno-Otero. 2006. Peginterferon-alfa2a plus ribavirin for 48 versus 72 weeks in patients with detectable hepatitis C virus RNA at week 4 of treatment. Gastroenterology 131:451–460.
38. Tong, M. J., N. S. el-Farra, A. R. Reikes, and R. L. Co. 1995. Clinical outcomes after transfusion-associated hepatitis C. N. Engl. J. Med. 332: 1463–1466.
39. Wakita, T., T. Pietschmann, T. Kato, T. Date, M. Miyamoto, Z. Zhao, K. Murthy, A. Habermann, H. G. Krausslich, M. Mizokami, R. Bartenschlager, and T. J. Liang. 2005. Production of infectious hepatitis C virus in tissue culture from a cloned viral genome. Nat. Med. 11:791–796.
40. Wasley, A., and M. J. Alter. 2000. Epidemiology of hepatitis C: geographic differences and temporal trends. Semin. Liver Dis. 20:1–16.
41. Watashi, K., M. Hijikata, M. Hosaka, M. Yamaji, and K. Shimotohno. 2003. Cyclosporin A suppresses replication of hepatitis C virus genome in cultured hepatocytes. Hepatology 38:1282–1288.
42. Watashi, K., N. Ishii, M. Hijikata, D. Inoue, T. Murata, Y. Miyanari, and K. Shimotohno. 2005. Cyclophilin B is a functional regulator of hepatitis C virus RNA polymerase. Mol. Cell 19:111–122.
43. Yeh, S. L., W. Y. Wang, C. S. Huang, and M. L. Hu. 2006. Flavonoids suppresses the enhancing effect of beta-carotene on DNA damage induced by 4-(methylnitrosamino)-1-(3-pyridyl)-1-butanone (NNK) in A549 cells. Chem. Biol. Interact. 160:175–182.
44. Yin, H., E. S. Musiek, L. Gao, N. A. Porter, and J. D. Morrow. 2005. Regiochemistry of neuroprostanes generated from the peroxidation of docosahexaenoic acid in vitro and in vivo. J. Biol. Chem. 280:26600–26611.
45. Zhong, J., P. Gastaminza, G. Cheng, S. Kapadia, T. Kato, D. R. Burton, S. F. Wieland, S. L. Uprichard, T. Wakita, and F. V. Chisari. 2005. Robust hepatitis C virus infection in vitro. Proc. Natl. Acad. Sci. USA 102:9294–9299.

ANTIMICROBIAL AGENTS AND CHEMOTHERAPY, Oct. 2007, p. 3756–3759 Vol. 51, No. 10
0066-4804/07/$08.00+0 doi:10.1128/AAC.00233-07

Identification of Novel Epoxide Inhibitors of Hepatitis C Virus Replication Using a High-Throughput Screen▽†§

Lee F. Peng,[1,2,3]‡ Sun Suk Kim,[1,4]‡ Sirinya Matchacheep,[2,3] Xiaoguang Lei,[5] Shun Su,[5] Wenyu Lin,[1] Weerawat Runguphan,[2,3] Won-Hyeok Choe,[1] Naoya Sakamoto,[6] Masanori Ikeda,[7] Nobuyuki Kato,[7] Aaron B. Beeler,[5] John A. Porco, Jr.,[5] Stuart L. Schreiber,[2,3,8] and Raymond T. Chung[1]*

GI Unit, Department of Medicine, Massachusetts General Hospital, 55 Fruit Street, Boston, Massachusetts 02114[1]; Department of Chemistry and Chemical Biology, Harvard University, 12 Oxford Street, Cambridge, Massachusetts 02138[2]; The Broad Institute of Harvard and MIT, 7 Cambridge Center, Cambridge, Massachusetts 02142[3]; Department of Gastroenterology and Hepatology, Gachon University Gil Medical Center, 1198 Guwol-dong, Namdong-gu, Incheon, 405-760 Korea[4]; Department of Chemistry and Center for Chemical Methodology and Library Development (CMLD-BU), Boston University, 590 Commonwealth Avenue, Boston, Massachusetts 02215[5]; Department of Gastroenterology and Hepatology, Tokyo Medical and Dental University, Tokyo, Japan[6]; Department of Molecular Biology, Okayama University Graduate School of Medicine, Dentistry, and Pharmaceutical Sciences, Okayama, Japan[7]; and Howard Hughes Medical Institute, Chevy Chase, Maryland[8]

Received 15 February 2007/Returned for modification 7 May 2007/Accepted 28 July 2007

Using our high-throughput hepatitis C replicon assay to screen a library of over 8,000 novel diversity-oriented synthesis (DOS) compounds, we identified several novel compounds that regulate hepatitis C virus (HCV) replication, including two libraries of epoxides that inhibit HCV replication (best 50% effective concentration, < 0.5 μM). We then synthesized an analog of these compounds with optimized activity.

Hepatitis C virus (HCV) infects over 170 million people worldwide and frequently leads to cirrhosis, liver failure, and hepatocellular carcinoma (1). Currently, the best therapy for the treatment of chronic hepatitis C is a combination of pegylated interferon and ribavirin, which has suboptimal efficacy and has an unfavorable side effect profile (14). The identification of more-effective and better-tolerated agents is therefore a high priority.

We have recently reported the successful adaptation of the Huh7/Rep-Feo replicon cell line (18) to a high-throughput screening assay system (8). Using this system, we previously screened a library of 2,568 well-known compounds whose biological activity is fully characterized (8). In order to discover novel regulators of HCV replication, we then screened a library of 8,064 diversity-oriented synthesis (DOS) compounds (15, 16). This library, known as the DOS set, is a

TABLE 1. Hits by library from the primary high-throughput screening with the DOS set[a]

Library	Increased luciferase signal hit libraries			Antiviral hit libraries		
	Hits	Members	Reference(s)	Hits	Members	Reference(s) or sources
FPA	11	319	5			
BUCMLD	4	880	10, 17	4	880	10, 17, Fig. 1, Table 2
JMM	4	544	13			
UGISS	1	319	2			
BUCMLD epoxyquinol				12	34	10, 17, Fig. 1 and 2, Table 2
SM				9	27	Fig. 1 and 2, Table 2
SpOx				6	612	6, 12
BEA				3	238	3
ICCB6				3	352	4
YKK				2	281	9
RTE				2	159	19

[a] The total number of compounds which comprise each library is listed in the "Members" columns.

* Corresponding author. Mailing address: GRJ 825A, GI Unit, Massachusetts General Hospital, Boston, MA 02114. Phone: (617) 724-7562. Fax: (617) 726-5895. E-mail: rtchung@partners.org.

† This publication is dedicated to Yoshito Kishi on the occasion of his 70th birthday.

§ Supplemental material for this article may be found at http://aac.asm.org/.

‡ L.F.P. and S.S.K. contributed equally to this project.

▽ Published ahead of print on 6 August 2007.

TABLE 2. Results of secondary screening with antiviral hit compounds from the SM and BUCMLD libraries[a]

Compound name	EC_{50}	CC_{50}
BUCMLD-B10A11	<0.5 (<0.5–0.5)	19.5 (19.4–22.4)
BUCMLD-B10A3	0.7 (<0.5–5.2)	9.0 (7.1–10.0)
BUCMLD-XL-184	1.4 (0.8–3.9)	>50
BUCMLD-B10A5	1.5 (<0.5–5.4)	39.3 (28.6–>50)
BUCMLD-XL-190	2.5 (<0.5–10)	>50
BUCMLD-B10A1	2.6 (1.0–5.0)	18.0 (15.9–19.5)
SM_A14B5	3.5 (2.7–4.4)	27.1 (18.0–44.6)
BUCMLD-XL-189	3.8 (2.2–7.0)	>50
SM_A6B5_2P100	6.6 (4.0–15.3)	>50
BUCMLD-B10A8	7.0 (0.9–30.0)	>50
BUCMLD-B10A10	7.0 (5.4–30.0)	>50
BUCMLD-B10A14	7.6 (1.0–23.0)	>50
BUCMLD-B10A7	7.75 (1.0–30.0)	35.3 (33.6–36.7)
SM_A4B6_2P123	8.0 (6.3–10.0)	>50
SM_A5B5_2P118	9.1 (2.5–16.7)	>50
SM_A7C2_2P155	12.7 (7.0–24.0)	>50
BUCMLD-B13A2	14.2 (6.4–45.0)	>50
SM_A1B2_1P32	19.6 (11.7–28.2)	>50
SM_A1B5_2P24	19.7 (6.25–50.0)	>50
BUCMLD-B13A1	21.1 (7.5–36.7)	>50
SM_A5B3_2P141	25.7 (18.3–39.8)	>50
SM_A5B2_2P142	26.7 (9.1–50.0)	>50
BUCMLD-NTM-EN2-67A	30.0 (0.7–46.1)	>50
SM_A12B3	>30	>50
BUCMLD-B10A13	42.9 (25.2–59.4)	>50
BUCMLD-XL-130	>100	>50

[a] Note that structure-activity relationship SM library compounds are also included. The EC_{50} and 50% cytotoxic concentration (CC_{50}) are reported in μM with 95% confidence intervals in parentheses. A value of <0.5 indicates a concentration of less than 0.5 μM; >30 indicates a concentration of greater than 30 μM; >50 indicates a concentration of greater than 50 μM; and >100 indicates a concentration of greater than 100 μM.

meta-library comprised of DOS libraries from chemists throughout the United States and Canada. Information about the DOS set is available at http://www.broad.harvard.edu/chembio/platform/screening/compound_libraries/index.htm.

The high-throughput primary screen and the secondary validation assays were performed as described in our previous publication (8).

Computational data analysis of the primary screening results was performed as previously described (8) except for the hit criteria. As the characteristics of this data set are different from those generated by our previous screen (8), different threshold values were chosen to assure optimal hit selection. Compounds were considered hits for inhibiting replication if they had a composite Z score of <-2.57 in the reporter gene screen, a reproducibility of >0.9 or <-0.9 in that screen, and a composite Z score of >-2.00 in the cell viability screen. Compounds were considered hits for stimulating luciferase production if they had a composite Z score of >2.50 in the reporter gene screen, a reproducibility of >0.9 or <-0.9 in that screen, and a composite Z score of <1.00 in the cell viability screen.

Full synthetic experimental procedures and spectroscopic data for the SM library compounds discussed in this publication are provided in the supplemental material. The synthesis of the full SM library, including compounds not discussed here, will be the subject of an upcoming report.

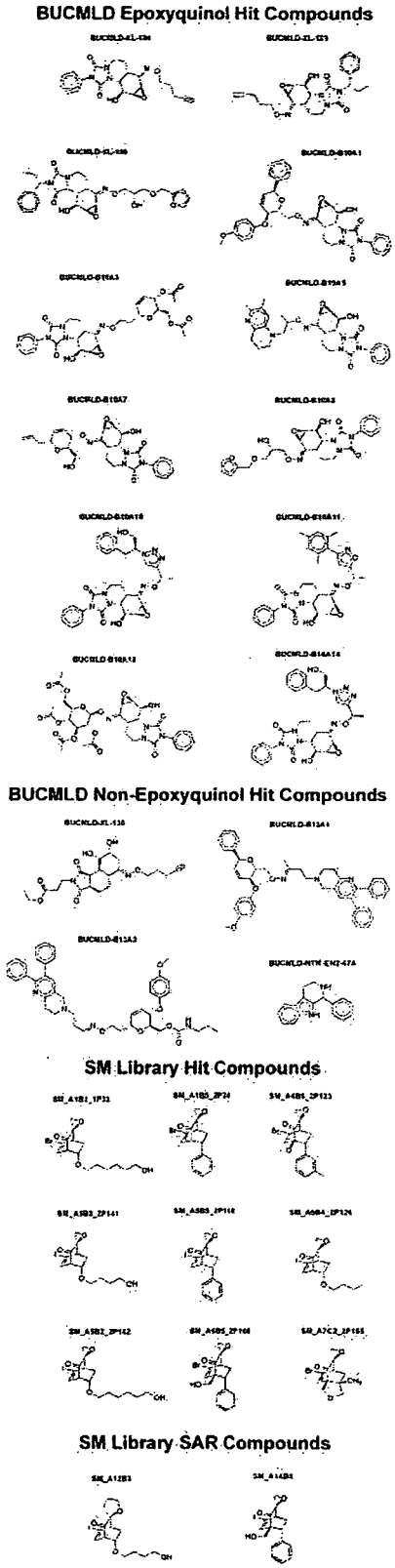

FIG. 1. Structures of antiviral hit compounds from the BUCMLD and SM libraries. SAR, structure-activity relationship.

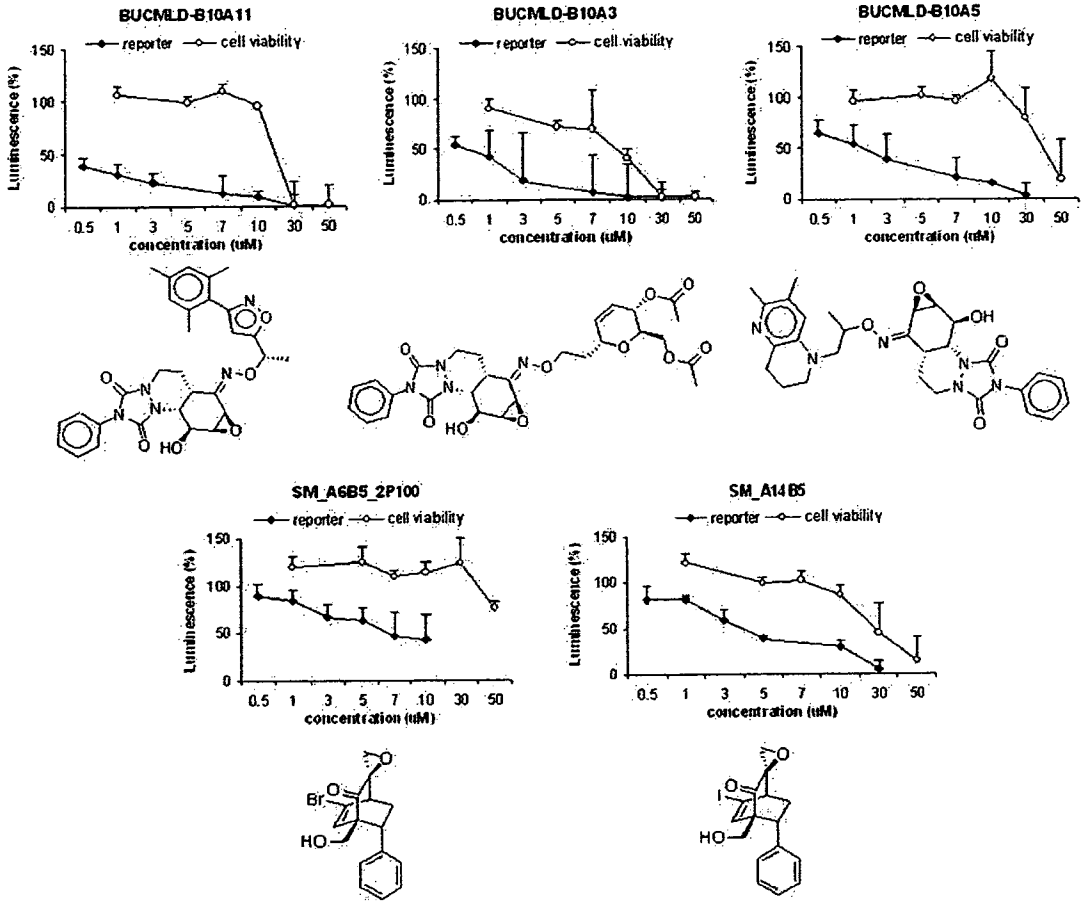

FIG. 2. Selected graphical results of secondary screening with antiviral hit compounds from the SM and BUCMLD epoxyquinol libraries. Luciferase activity for HCV RNA replication levels is shown as a percentage of control. Cell viability is also shown as a percentage of control. Each point represents the average of triplicate data points with standard deviation represented as the error bar.

The synthesis of the BUCMLD epoxyquinol library has been previously described (10, 17).

Full experimental details regarding the JFH1 HCVcc system (11) are provided in the supplemental material. We identified 41 antiviral compounds that inhibited HCV replication and 20 proviral compounds that increased luciferase production (Table 1). In our analysis of the antiviral hit compounds from the DOS set, a striking finding was that 21 of the 41 compounds contained an epoxide moiety. Moreover, the most potent of these compounds were epoxides. Further analysis revealed that these epoxides came from only two DOS libraries, SM and BUCMLD epoxyquinol (10, 17), with very high sublibrary hit rates of 35% and 33%, respectively (Table 1). Of note, the non-hit members of these two libraries did exhibit antiviral activity but failed to meet the formal hit criteria.

As we were especially intrigued by these epoxide-bearing compounds, we restricted our hit validation to these compounds (Table 2 and Fig. 1). SM_A6B5_2P100 was the most active member of the SM library, while BUCMLD-B10A11 was the most potent member of the BUCMLD epoxyquinol library (Table 2 and Fig. 2).

Structure-activity relationship analysis of the SM library reveals the structural elements most important for antiviral activity (Table 2 and Fig. 1). Comparing SM_A5B5_2P118 to SM_A1B5_2P24, iodinated compounds are more active than brominated ones. Comparing SM_A5B5_2P118 to SM_A5B3_2P141 and SM_A5B2_2P142, compounds with a phenyl substituent are more active than those with aliphatic chains. Finally, the most active compounds, SM_A4B6_2P123 and SM_A6B5_2P100, have a bridgehead substituent. Thus, we hypothesized that the most active compound should bear an iodine, a phenyl substituent, and a bridgehead substituent.

SM_A14B5, which incorporates all of these elements, was therefore synthesized, as it was reasoned to be the most active SM library compound. Indeed, SM_A14B5 had a 50% effective concentration (EC_{50}) of approximately 3.5 μM, which is about half that of SM_A6B5_2P100 (Table 2 and Fig. 2).

The most potent compounds from each library, SM_A14B5 and BUCMLD-B10A11, underwent further validation in the infectious JFH1 HCVcc system (11). They were tested at concentrations of 5 μM and 1 μM, respectively, and inhibited HCV replication 48.4% ± 5.9% and 45.1% ± 5.2%, respectively, relative to the level of inhibition achieved by interferon at a concentration of 1 ng/ml. These data roughly approximate the EC_{50} validation data derived from the OR6 system (7) in

which inhibition was also measured relative to that of interferon at a concentration of 1 ng/ml.

Our observations suggest that the epoxide moiety is essential for potent antiviral activity. Analyzing the BUCMLD compounds, those compounds that bear an epoxide moiety are, in general, more-potent antivirals than those that do not (Table 2 and Fig. 1). Furthermore, all of the compounds from the SM library bear epoxides. SM_A12B3, an analog of SM_A5B3_2P141, which bears a tetrahydrofuran moiety in place of an epoxide, was therefore synthesized to further test this hypothesis. SM_A12B3 had negligible antiviral activity (Table 2), while SM_A5B3_2P141 displayed modest antiviral activity. Other analogs of SM compounds bearing tetrahydrofuran rings in place of epoxides showed similar attenuation of antiviral activity relative to their parent compounds. Unfortunately, attempts to synthesize the tetrahydrofuran analog of the most potent SM compound, SM_A14B5, have so far been unsuccessful.

It is interesting to note that it is the urazole-containing epoxyquinol constituents of the BUCMLD epoxyquinol library, rather than the maleimide-derived ones, that demonstrated anti-HCV activity in the primary screen. It is therefore likely that the combination of a urazole with the epoxide is necessary for the activity of the BUCMLD epoxyquinol compounds.

Although none of our most potent antiviral DOS compounds showed significant cytotoxicity at their EC_{50}s, all of them ultimately proved to be cytotoxic at higher concentrations (Table 2 and Fig. 2). Therefore, future modifications should not only aim to improve anti-HCV activity but should also attempt to decrease cytotoxicity, in order to widen the therapeutic window.

It is tempting to hypothesize that these epoxides exert their antiviral effects through a common pathway. Presumably, they act as electrophiles, with the nucleophilic target making a covalent bond by attacking and opening the epoxides. Studies to elucidate their mechanism of action are under way.

We thank the National Cancer Institute and the Initiative for Chemical Genetics, who provided support for this publication, and the Chemical Biology Platform of the Broad Institute of Harvard and MIT for their assistance in this work.

The project has been funded in whole or in part with federal funds from the National Cancer Institute's Initiative for Chemical Genetics, National Institutes of Health, under contract no. N01-CO-12400.

The content of this publication does not necessarily reflect the views or policies of the Department of Health and Human Services, nor does mention of trade names, commercial products, or organizations imply endorsement by the U.S. government.

Financial support was provided by the following: The American Gastroenterological Association FDHN/TAP Pharmaceuticals FFT Award (L.F.P.), The GlaxoSmithKline Research Fund of the Korean Association for The Study of The Liver (S.S.K.), NIH 5T32DK07191-31 (L.F.P.), NIH NS050854-01 (R.T.C.), and the NIGMS CMLD Initiative P50 GM067041 (J.A.P.).

REFERENCES

1. **Alter, M. J.** 2006. Epidemiology of hepatitis C. Hepatology **43**:S207–S220.
2. **Andreana, P. R., C. C. Liu, and S. L. Schreiber.** 2004. Stereochemical control of the Passerini reaction. Org. Lett. **6**:4231–4233.
3. **Brittain, D. E. A., B. L. Gray, and S. L. Schreiber.** 2005. From solution-phase to solid-phase enyne metathesis: crossover in the relative performance of two commonly used ruthenium pre-catalysts. Chem. Eur. J. **11**:5086–5093.
4. **Burke, M. D., E. M. Berger, and S. L. Schreiber.** 2004. A synthesis strategy yielding skeletally diverse small molecules combinatorially. J. Am. Chem. Soc. **126**:14095–14104.
5. **Chen, C., X. Li, C. Neumann, M. M.-C. Lo, and S. L. Schreiber.** 2005. Convergent diversity-oriented synthesis of small-molecule hybrids. Angew. Chem. **117**:2–4.
6. **Chen, C., X. Li, and S. L. Schreiber.** 2003. Catalytic asymmetric [3+2] cycloaddition of azomethine ylides. Development of a versatile stepwise, three-component reaction for diversity-oriented synthesis. J. Am. Chem. Soc. **125**:10174–10175.
7. **Ikeda, M., K. Abe, H. Dansako, T. Nakamura, K. Naka, and N. Kato.** 2005. Efficient replication of a full-length hepatitis C virus genome, strain O, in cell culture, and development of a luciferase reporter system. Biochem. Biophys. Res. Commun. **329**:1350–1359.
8. **Kim, S. S., L. F. Peng, W. Lin, W.-H. Choe, N. Sakamoto, S. L. Schreiber, and R. T. Chung.** 2007. A cell-based, high-throughput screen for small molecule regulators of HCV replication. Gastroenterology **132**:311–320.
9. **Kim, Y.-K., M. A. Arai, T. Arai, J. O. Lamenzo, E. F. Dean, N. Patterson, P. A. Clemons, and S. L. Schreiber.** 2004. Relationship of stereochemical and skeletal diversity of small molecules to cellular measurement space. J. Am. Chem. Soc. **126**:14740–14745.
10. **Lei, X., N. Zaarur, M. Y. Sherman, and J. A. Porco.** 2005. Stereocontrolled synthesis of a complex library via elaboration of angular epoxyquinol scaffolds. J. Org. Chem. **70**:6474–6483.
11. **Lindenbach, B. D., M. J. Evans, A. J. Syder, B. Wolk, T. L. Tellinghuisen, C. C. Liu, T. Maruyama, R. O. Hynes, D. R. Burton, J. A. McKeating, and C. M. Rice.** 2005. Complete replication of hepatitis C virus in cell culture. Science **309**:623–626.
12. **Lo, M. M.-C., C. S. Neumann, S. Nagayama, E. O. Perlstein, and S. L. Schreiber.** 2004. A library of spirooxindoles based on a stereoselective three-component coupling reaction. J. Am. Chem. Soc. **126**:16077–16086.
13. **Mitchell, J. M., and J. T. Shaw.** 2006. A structurally diverse library of polycyclic lactams resulting from systematic placement of proximal functional groups. Angew. Chem. **45**:1722–1726.
14. **Pawlotsky, J. M.** 1997. Therapy of hepatitis C: from empiricism to eradication. Hepatology **26**:S62–S65.
15. **Schreiber, S. L.** 2000. Target-oriented and diversity-oriented organic synthesis in drug discovery. Science **287**:1964–1969.
16. **Schreiber, S. L.** 2003. Chemical genetics. Chem. Eng. News **81**:51–61.
17. **Su, S., D. E. Acquilano, J. Arumugasamy, A. B. Beeler, E. L. Eastwood, J. R. Giguere, P. Lan, X. Lei, G. K. Min, A. R. Yeager, Y. Zhou, J. S. Panek, J. K. Snyder, S. E. Schaus, and J. A. Porco.** 2005. Convergent synthesis of a complex oxime library using chemical domain shuffling. Org. Lett. **7**:2751–2754.
18. **Tanabe, Y., N. Sakamoto, N. Enomoto, M. Kurosaki, E. Ueda, S. Maekawa, T. Yamashiro, M. Nakagawa, C. H. Chen, N. Kanazawa, S. Kakinuma, and M. Watanabe.** 2004. Synergistic inhibition of intracellular hepatitis C virus replication by combination of ribavirin and interferon. J. Infect. Dis. **189**:1129–1139.
19. **Taylor, A. M., and S. L. Schreiber.** 2006. Enantioselective addition of terminal alkynes to isolated isoquinoline iminiums. Org. Lett. **8**:143–146.

Spatiotemporal Mobilization of Toll/IL-1 Receptor Domain-Containing Adaptor Molecule-1 in Response to dsRNA[1]

Kenji Funami,[2]* Miwa Sasai,[3]* Yusuke Ohba,† Hiroyuki Oshiumi,* Tsukasa Seya,* and Misako Matsumoto[4]*

TLR3 recognizes viral dsRNA and induces antiviral immune responses. TLR3-mediated cell activation relies on Toll/IL-1R (TIR) domain-containing adaptor molecule-1 (TICAM-1, also named TIR domain-containing adaptor inducing IFN-β or TRIF), which recruits downstream signaling molecules to activate the transcription factors IFN regulatory factor 3 (IRF-3) and NF-κB. The mechanisms by which TICAM-1 is activated and transmits signals remain largely unknown. In this study we show that TICAM-1 alters its distribution profile from a diffuse cytoplasmic form to a speckle-like structure in response to dsRNA. The receptor-interacting protein 1 (RIP1), a crucial signaling molecule for TICAM-1-mediated NF-κB activation, accumulated in the TICAM-1 speckles. In addition, NF-κB-activating kinase-associated protein 1 (NAP1), a downstream molecule linking TICAM-1 and the IRF-3-activating kinase TBK1 (TANK-binding kinase 1), was also recruited to the TICAM-1 speckles. Notably, a transient colocalization of TICAM-1 and TLR3 was observed before the extensive formation of the TICAM-1 speckles. Thus, the spatiotemporal mobilization of TICAM-1 in response to dsRNA and the formation of the TICAM-1 speckles containing RIP1 and NAP1 are important for the activation of the TLR3-TICAM-1 pathway. ***The Journal of Immunology,*** **2007, 179: 6867–6872.**

The innate immune system acts as the first line of defense against numerous pathogens. Both membrane-bound and cytoplasmic receptors recognize pathogen-associated molecular patterns and induce a multiple array of antimicrobial immune responses (1). TLR3 and cytoplasmic retinoic acid-inducible gene I (RIG)-like receptors recognize viral dsRNA (2–4). TLR3 detects extracellular dsRNA, the mode being distinct from that of a cytoplasmic RIG-like receptor. TLR3-mediated signaling relies on the downstream adaptor molecule Toll/IL-1R (TIR)[5] domain-containing adaptor molecule 1 (TICAM-1) (also called TIR domain-containing adaptor inducing IFN-β or TRIF), which activates the transcription factors IFN regulatory factor 3 (IRF-3), NF-κB, and MAPK, leading to the induction of type I IFN (especially IFN-β), cytokine/chemokine production, and dendritic cell (DC) maturation (5, 6).

Human TLR3 is predominantly expressed intracellularly in myeloid DCs and epithelial cells but not in plasmacytoid DCs (7, 8). TLR3 signaling arises in the intracellular compartment, but the mechanisms by which TICAM-1 transmits signals are still unclear. TICAM-1 possesses a proline-rich N-terminal region, a TIR domain, and a C-terminal region. The TIR domain of TICAM-1 is essential for binding to the TIR domain of TLR3 and also to the TLR4 adaptor TICAM-2 (also called TRIF-related adaptor molecule (TRAM)) (9, 10). Once TICAM-1 is oligomerized, the serine-threonine kinases TANK-binding kinase 1 (TBK1; also called NAK or T2K) and IκB kinase-related kinase ε (IKK-ε; also called IKK-i), are activated and phosphorylate IRF-3 (11, 12). NF-κB-activating kinase-associated protein 1 (NAP1) participates in the recruitment of these kinases to the N-terminal region of TICAM-1 (13). Whereas the N-terminal region is crucial for TICAM-1-mediated IRF-3 activation, the C-terminal region of TICAM-1 is involved in NF-κB activation and apoptosis. It has been accepted that receptor-interacting protein 1 (RIP1), a kinase containing a death domain, associates with TICAM-1 via the RIP homotypic interaction motif (RHIM) domain in the C-terminal region and acts as an NF-κB inducer and apoptosis mediator in TICAM-1-mediated signaling (14–16).

In contrast to other TLR adaptors, overexpression of TICAM-1 leads to the induction of IFN-β promoter activation and apoptosis. We therefore surmised that the TICAM-1 signaling is initiated apart from TLR3. In this study, we examined the subcellular localization of TICAM-1 in comparison with TLR3 and other

*Department of Microbiology and Immunology, and †Department of Pathophysiology and Signal Transduction, Department of Pathology, Hokkaido University Graduate School of Medicine, Kita-ku Sapporo, Japan

Received for publication July 13, 2007. Accepted for publication September 11, 2007.

The costs of publication of this article were defrayed in part by the payment of page charges. This article must therefore be hereby marked *advertisement* in accordance with 18 U.S.C. Section 1734 solely to indicate this fact.

[1] This work was supported in part by Core Research for Engineering, Science, and Technology (CREST), JST (Japan Science and Technology Corporation (JST), grants-in-aid from the Ministry of Education, Science, Sports, and Culture (Specified Project for Advanced Research) and the Hepatitis C Virus (HCV) Project of the National Institute of Health (NIH) of Japan, and by the Uehara Memorial Foundation, Mitsubishi Foundation, Takeda Foundation, and Northtec Foundation.

[2] Current address: Center for Integrated Medical Research, Keio University, Tokyo, Japan.

[3] Current address: Department of Immunobiology, Yale University School of Medicine, New Haven, CT 06510.

[4] Address correspondence and reprint requests to Dr. Misako Matsumoto, Department of Microbiology and Immunology, Hokkaido University Graduate School of Medicine, Kita 15, Nishi 7, Kita-ku Sapporo, Japan. E-mail address: matumoto@pop.med.hokudai.ac.jp

[5] Abbreviations used in this paper: TIR, Toll/IL-1 receptor; CFP, cyan fluorescent protein; DAPI, 4′,6′-diamidino-2-phenylindole; DC, dendritic cell; EEA1, early endosome Ag 1; FRET, fluorescence resonance energy transfer; FRET^C, corrected FRET; IRF-3, IFN regulatory factor 3; MPR, mannose-6-phosphate receptor; NAP1, NF-κB activating kinase-associated protein 1; pAb, polyclonal Ab; poly(I:C), polyinosinic/polycytidylic acid; PGN, peptidoglycan; RIP1, receptor-interacting protein 1; TICAM-1, TIR domain-containing adaptor molecule 1; TRAM, TRIF-related adaptor molecule; TRIF, TIR domain-containing adaptor inducing IFN-β; YFP, yellow fluorescent protein; z-VAD-fmk, benzyloxycarbonyl-Val-Ala-Asp-fluoromethyl ketone.

signaling molecules in human epithelial cell lines by live cell imaging and confocal immunofluorescence analyses. TICAM-1 appears to be mobile depending on the activation state of its coupling receptor, TLR3. Here we demonstrated that TICAM-1 alters the distribution profile concomitant with its activation from a diffuse cytoplasmic form to a speckle-like structure containing RIP1 and NAP1 where TICAM-1-mediated signaling is initiated.

Materials and Methods

Reagents and cell culture

Anti-human TLR3 mAb (clone TLR3.7) was generated in our laboratory (3). Anti-RIP1 and anti-IRF-3 mAbs were purchased from BD Biosciences. Anti-early endosome Ag 1 (EEA1) polyclonal Ab (pAb) was from Affinity Bioreagents, anti-calnexin pAb was from StressGen Biotechnologies, anti-FLAG M2 mAb, anti-HA pAb, 4′,6′-diamidino-2-phenylindole (DAPI) dihydrochloride and benzyloxycarbonyl-Val-Ala-Asp-fluoromethyl ketone (z-VAD-fmk) were from Sigma-Aldrich, anti-mannose-6-phosphate receptor (MPR) pAb was from Abcam, anti-Myc mAb was from NeoMarkers (Lab Vision), and anti-p115 pAb was from Calbiochem. LysoTracker Red DND-99 and Alexa Fluor 488- and Alexa Fluor 568-conjugated secondary Abs were from Invitrogen Life Technologies. Polyriboinosinic/polyribocytidylic acid (poly(I:C)) was from Amersham Biosciences, and peptidoglycan (PGN) from *Staphylococcus aureus* was from Fluka Chemie. Rabbit anti-human TICAM-1 pAb was generated in our laboratory using recombinant TICAM-1 (aa 1–361) as the immunogen. HeLa cells were maintained in MEM (Nissui Pharmaceutical) supplemented with 10% heat-inactivated FCS (Invitrogen Life Technologies).

Plasmids

Complementary DNAs for human TLR3, TICAM-1, and RIP1 were cloned in our laboratory by RT-PCR and ligated at the cloning site of the expression vector, pFLAG-CMV, pEF-BOS, p3xFLAG14 (C-terminal 3xFLAG tag), pECFP-N1 (C-terminal cyan fluorescent protein (CFP) tag), or pEYFP-N1 (C-terminal yellow fluorescent protein (YFP) tag). pECFP-C1 (N-terminal CFP tag) was used to make TICAM-1 tagged with CFP. cDNAs of NAP1 were kindly provided by Dr. M. Nakanishi (Nagoya City University, Nagoya, Japan).

Confocal microscopy

HeLa cells (1.0×10^5 cells/well) were plated onto a micro cover glass (Matsunami Glass) in a 24-well plate. The following day, cells were transfected with the indicated plasmids using Lipofectamine Plus (Invitrogen Life Technologies) or FuGENE HD (Roche). The total amounts of DNA were kept constant by adding empty vector. In some cases transfection was performed in the presence of z-VAD-fmk (final concentration, 20 μM) to inhibit apoptosis. After 24 h (under the presence of z-VAD-fmk) or 12 h (under the absence of z-VAD-fmk), cells were fixed in acetone or 1% formaldehyde in PBS. In the case of formaldehyde fixation, cells were then permeabilized with PBS containing 0.2% Triton X-100 for 15 min. Fixed cells were blocked in PBS containing 1% BSA and labeled with the indicated primary Abs for 1 h at room temperature. Alexa Fluor 488- or Alexa Fluor 568-conjugated secondary Abs (×400 dilution) were used for the visualizing staining of the primary Abs. For acidic organelle staining, cells were treated with LysoTracker (500 μM) for 30 min before fixation. For nucleus staining, cells were treated with DAPI (final concentration, 2 μg/ml) in PBS for 10 min before mounting. After all staining procedures were finished, micro cover glasses were mounted onto a slide glass using PBS containing 2.3% 1,4-diazabicyclo[2.2.2]octane (DABCO) and 50% glycerol. Cells were visualized at ×63 magnification under an LSM510 META microscope (Zeiss).

Time lapse analysis

Time-lapse analyses were performed using AquaCosmos 2.0 software (Hamamatsu Photonics) to control a digital imaging system coupled to an inverted microscope (IX-70; Olympus). Briefly, HeLa cells (5×10^5/dish) were plated onto a 36-mm glass dish (IWAKI; Gene Company). The following day, cells were transfected with indicated plasmid using FuGENE HD (Roche) in the presence of z-VAD-fmk. The total amount of DNA (2 μg) was kept constant by adding empty vector. After 18–24 h from transfection, cells were stimulated with 20 μg/ml poly(I:C) or PGN for the indicated times and images were acquired through a cooled charge-coupled device camera (ORCA ER; Hamamatsu Photonics).

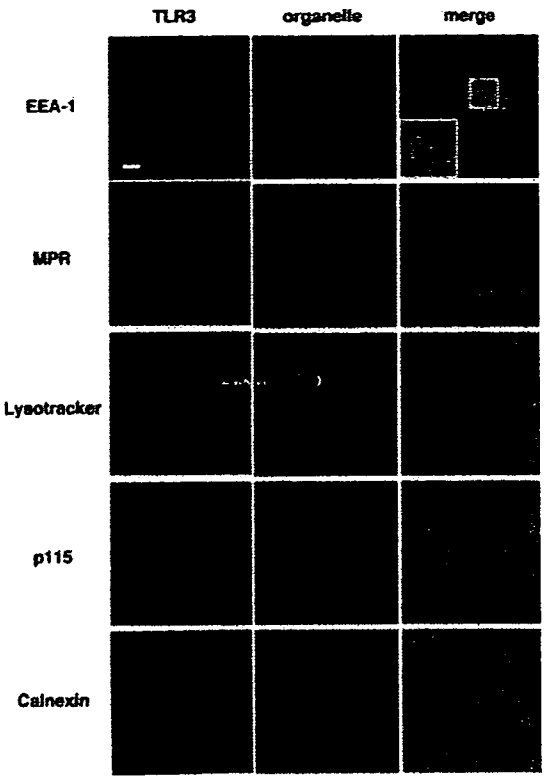

FIGURE 1. Subcellular localization of TLR3 in epithelial cell lines. Endogenous TLR3 partly localizes to the early endosome in HeLa cells. Cells were stained with TLR3.7 (20 μg/ml) followed by an Alexa Fluor 488-conjugated secondary Ab. Organelles were stained with anti-EEA1 pAb (2 μg/ml), anti-MPR pAb (10 μg/ml), anti-p115 pAb (3 μg/ml), or anti-calnexin pAb (×200 dilution) followed by an Alexa Fluor 568-conjugated secondary Ab. For LysoTracker staining, cells were pretreated with 500 nM LysoTracker Red for 30 min before fixation (red). Confocal images are shown. The *inset* in the lower left corner of the EEA-1 merge panel shows a ×2-magnified image of the smaller white-boxed area. Green, TLR3; red, organelle markers; blue, nuclei with DAPI; bar, 10 μm.

Fluorescence resonance energy transfer (FRET) analysis

The sensitized FRET measurement was performed as described previously (17). Fluorescent images were acquired sequentially through YFP, CFP, and FRET filter channels. Filter sets used were YFP (excitation, 500/25 nm; emission, 535/26 nm), CFP (excitation, 440/21 nm; emission, 480/30 nm), and FRET (excitation, 440/21 nm; emission, 535/26 nm). An XF2034 (455DRLP) dichroic mirror was used throughout the experiments. Integration times were 100–200 ms with a 2×2 binning mode. The background was subtracted from raw images before FRET calculations. Corrected FRET ($FRET^C$) was calculated on a pixel-by-pixel basis for the entire image using the following equation: $FRET^C = FRET - (a \times CFP) - (b \times YFP)$, where FRET, YFP, and CFP correspond to background-subtracted images of cells coexpressing CFP and YFP acquired through the FRET, YFP, and CFP channels, respectively. a and b are the fractions of bleed-through of CFP and YFP fluorescences, respectively, through the FRET channel that were ordinarily 0.52 and 0.48, respectively, under our experimental conditions.

Reporter gene assay

HeLa cells in a 96-well plate were transiently transfected with the expression vector for $TICAM\text{-}1^{YFP}$ (0.1 ng, 10 ng) or empty vector together with p-125 Luc reporter plasmid (15 ng) and an internal control vector, phRL-TK (0.5 ng) using FuGENE HD. The p-125 Luc reporter that contains the human IFN-β promoter region (−125 to + 19) was provided by Dr. T. Taniguchi (University of Tokyo, Tokyo, Japan). The total amount of DNA (100 ng) was kept constant by adding empty vector. After 24 h, cells were lysed in lysis buffer (Promega) and firefly and *Renilla* luciferase activities were determined according to the manufacturer's instructions. Luciferase activity was normalized by *Renilla* luciferase activity and expressed as the fold stimulation relative to the activity in vector-transfected cells.

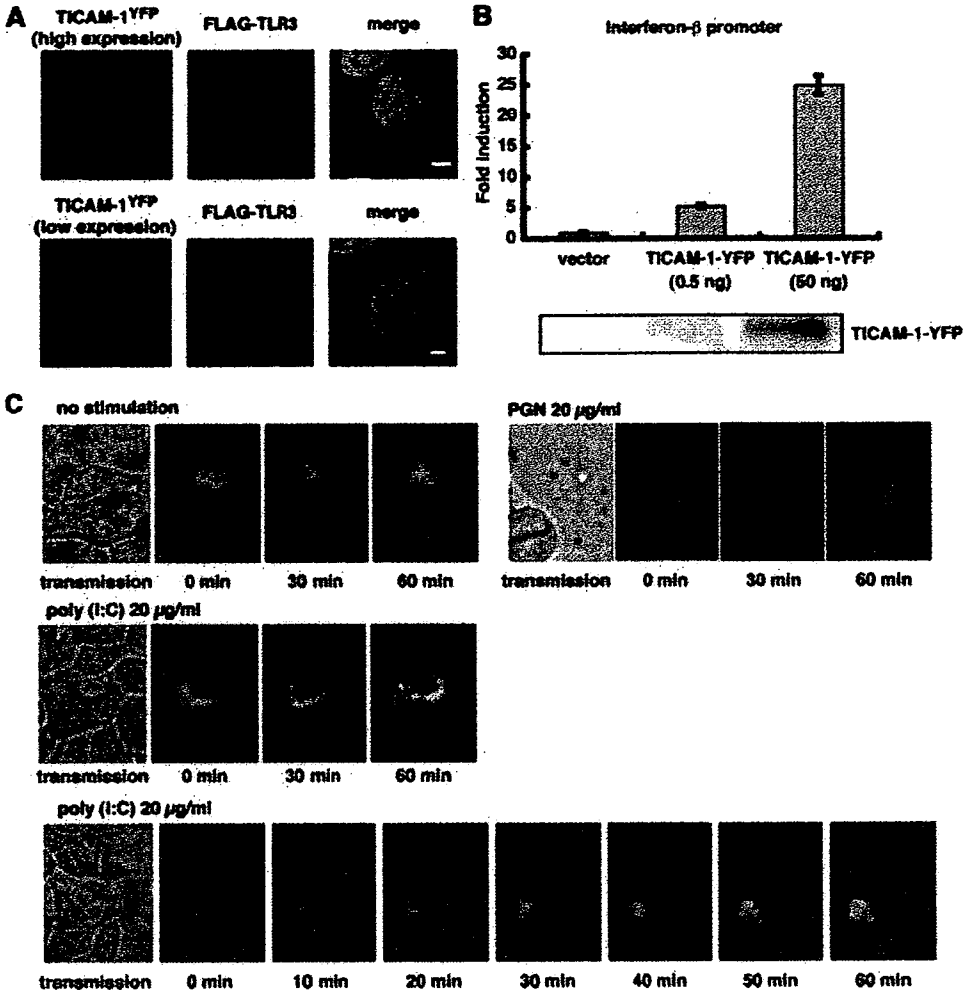

FIGURE 2. The distribution profile of TICAM-1 alters in response to poly(I:C). *A*, Confocal images of HeLa cells coexpressing TICAM-1^{YFP} and FLAG-TLR3. HeLa cells in a 24-well plate were cotransfected with TICAM-1^{YFP} (50 ng for high expression, 0.5 ng for low expression) and FLAG-TLR3 (250 ng) using FuGENE HD in the presence of Z-VAD-fmk. The total amount of DNA (500 ng) was kept constant by adding empty vector. After 24 h the cells were fixed and TLR3 was stained with anti-FLAG mAb and Alexa Fluor 568-conjugated secondary Ab. *Upper panels*, HeLa cells were transfected with a high dose of the TICAM-1 plasmid. TICAM-1^{YFP} forms speckle-like structures in the cytosol. *Lower panels*, HeLa cells were transfected with a low dose of the TICAM-1 plasmid. TICAM-1^{YFP} localizes diffusely in the cytosol. Green, TICAM-1^{YFP}; red, FLAG-TLR3; blue, nuclei with DAPI; bar, 10 μm. *B*, *Upper panel*, Luciferase reporter activity of TICAM-1^{YFP}. HeLa cells in a 24-well plate were transiently transfected with TICAM-1^{YFP} plasmid (0.5 ng or 50 ng/well) or empty vector together with the p-125-Luc reporter plasmid and the phRL-TK reporter plasmid using FuGENE HD. After 24 h, luciferase activities were measured and expressed as the fold stimulation relative to the activity in vector-transfected cells. Representative data from a minimum of three separate experiments are shown. *Lower panel*, Protein expression of TICAM-1^{YFP} was assessed by immunoblotting with anti-TICAM-1 pAb. *C*, TICAM-1 forms speckle-like structures in response to poly(I:C). HeLa cells expressing a low level of TICAM-1^{YFP} were placed on a time-lapse microscope and stimulated with poly(I:C) (20 μg/ml) (*center* and *lower panels*) or PGN (20 μg/ml) (*upper right panels*) for up to 60 min or left unstimulated (*upper left panels*). Cell images were taken every 10 min. YFP images at the indicated periods are shown.

Immunoblotting

HeLa cells (1×10^5 cells/well) in a 24-well plate were transfected with TICAM-1^{YFP} plasmid (0.5, 50 ng) or empty vector using FuGENE HD in the presence of z-VAD-fmk. The total amount of DNA (500 ng) was kept constant by adding empty vector. After 24 h, cells were lysed in lysis buffer (20 mM Tris-HCl (pH 7.5) containing 150 mM NaCl, 1% Nonidet P-40, 10 mM EDTA, 25 mM iodoacetamide, 2 mM PMSF, and protease inhibitor mixture (Roche)) and subjected to SDS-PAGE (10%) under reducing conditions, followed by immunoblotting with rabbit anti-TICAM-1 pAb.

Results

TLR3 localizes to the early endosome in the human epithelial cell line HeLa

We previously showed that TLR3 localizes to intracellular compartments in human monocyte-derived DCs (7). To identify the organelle in which TLR3 resides, we extended the analysis of the subcellular localization of endogenous TLR3 in HeLa cells with a low level of expression of TLR3 on the plasma membrane and a higher level of expression in intracellular organelles. TLR3-positive compartments were partially merged with EEA1 (Fig. 1). Late endosome (MPR), lysosome (LysoTracker), Golgi (p115), and endoplasmic reticulum (calnexin) markers were not colocalized with TLR3. Thus, in steady-state conditions some TLR3 molecules localize to the early endosome in epithelial cells, consistent with a previous study (18).

TICAM-1 alters the distribution profile in the cytosol in response to dsRNA

To clarify how TLR3 transmits signals to the adaptor protein TICAM-1, we analyzed the subcellular localization of TICAM-1 in HeLa cells. To visualize the expression of TICAM-1, we prepared a TICAM-1 construct tagged with YFP, TICAM-1^{YFP}, which

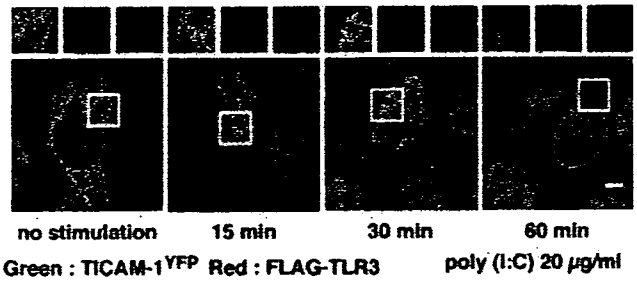

FIGURE 3. Transient association of TICAM-1 with TLR3 in response to poly(I:C). Confocal images of HeLa cells coexpressing TICAM^{YFP} with FLAG-TLR3 are shown. HeLa cells were cotransfected with TICAM^{YFP} and FLAG-TLR3 and stimulated with poly(I:C) (20 μg/ml) for up to 60 min. At the indicated periods, cells were fixed and stained with anti-FLAG mAb (5 μg/ml) and Alexa Fluor 568-conjugated secondary Ab. *Upper panels* show ×1.5 magnified images of the *insets* in the *lower panels*. Green, TICAM-1^{YFP}; red, FLAG-TLR3; blue, nuclei with DAPI; bar, 10 μm.

possesses IRF-3- and NF-κB- activating abilities. We first coexpressed FLAG-tagged TLR3 and TICAM-1^{YFP} in HeLa cells and subjected these cells to confocal microscopic analysis. As shown in Fig. 2*A*, overexpressed TICAM-1 was localized to the speckle-like structures in the cytosol and did not colocalize with TLR3 (*upper panels*). Because overexpressed TICAM-1 induces apoptosis in a caspase-dependent manner, transfected cells were cultured in the presence of a caspase inhibitor (z-VAD-fmk) for 24 h or cultured for only <12 h in the absence of z-VAD-fmk. Under both cell culture conditions TICAM-1 formed a speckle-like localization pattern (data not shown). In contrast, by transfecting a limited dose of the TICAM-1 plasmid into HeLa cells TICAM-1 emerged diffusely in the cytosol and did not colocalize with TLR3 (Fig. 2*A*, *lower panels*). In this experimental condition, TICAM-1^{YFP} protein level was so low that it only weekly activated the IFN-β promoter (Fig. 2*B*, *middle column*). In contrast, when cells were transfected with a high dose of the TICAM-1^{YFP} plasmid, the TICAM-1^{YFP} protein level was sufficiently high to induce IFN-β promoter activation (Fig. 2*B*, *right column*). It has been found that overexpressed TICAM-1 strongly induces IFN-β promoter activation in HEK293 cells irrespective of TLR3 stimulation (5, 19). We therefore hypothesized that the distribution profile of TICAM-1 depends on its activation stage. To test this issue, HeLa cells expressing a low level of TICAM-1^{YFP} were stimulated with poly(I:C), a synthetic dsRNA, and subjected to a time-lapse analysis using an inverted fluorescence microscope. In response to poly(I:C), TICAM-1^{YFP} formed speckle-like structures in a time-dependent manner (Fig. 2*C*, *middle* and *lower panels*). The speckle-like structures appeared 30 min after poly(I:C) stimulation and were gradually increased and concentrated. The tendency of TICAM-1 to form speckles increased to a level comparable to that of overexpression. In the absence of poly(I:C), TICAM-1 remained diffuse in the cytosol (Fig. 2*C*, *upper left panels*). Also, TICAM-1 did not alter the distribution profile upon PGN (TLR2 ligand) stimulation, suggesting that TICAM-1 speckle formation specifically depends on TLR3 stimulation (Fig. 2*C*, *upper right panels*).

Transient colocalization of TICAM-1 and TLR3 in response to dsRNA

When poly(I:C) is exogenously added to the cells it is delivered to the intracellular compartments in which TLR3 resides and activates the latter (20, 21). To visualize the association of TICAM-1 with TLR3 upon poly(I:C) stimulation, HeLa cells were cotransfected with TICAM-1^{YFP} and FLAG-TLR3 and stimulated with poly(I:C) for 60 min. Cells were subjected to confocal immunofluorescence analyses. TICAM-1 and TLR3 were localized distinctly in unstimulated cells (Fig. 3). Partial colocalization of TICAM-1 and TLR3 was observed within 30 min after poly(I:C) stimulation. However, 60 min after poly(I:C) stimulation TICAM-1 dissociated from TLR3, forming speckles. Hence, TICAM-1 in the cytosol is transiently recruited to the endosomal TLR3 in response to dsRNA and thereafter moves away from TLR3 to form speckle-like structures.

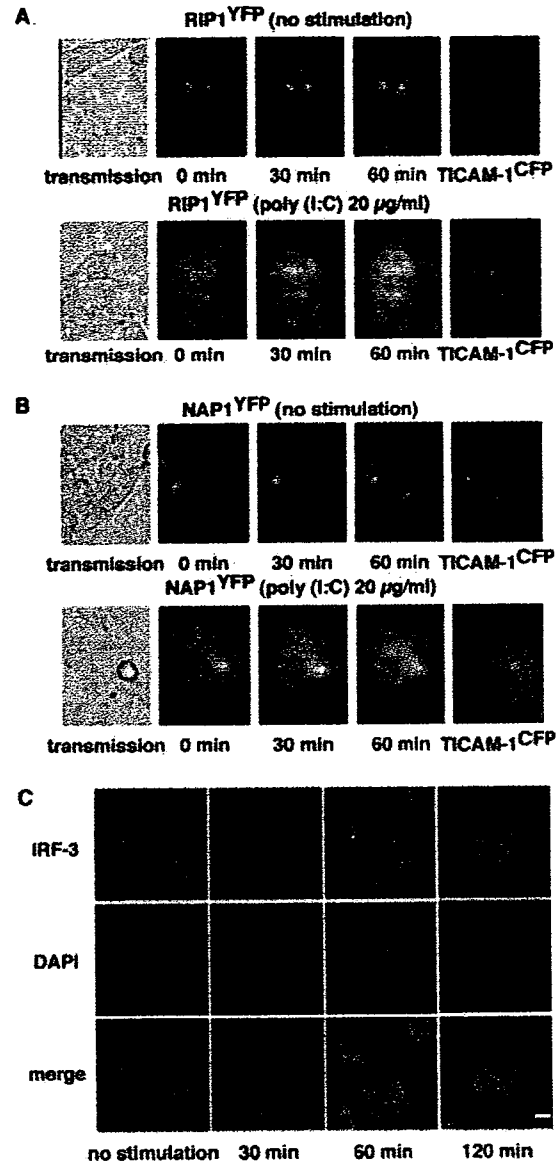

FIGURE 4. Subcellular localization of RIP1, NAP1, and IRF-3. *A* and *B*, RIP1 and NAP1 accumulate in the speckle-like structures in response to poly(I:C). HeLa cells coexpressing RIP1^{YFP} (*A*) or NAP1^{YFP} (*B*) with TICAM-1^{CFP} were placed on a time-lapse microscope and imaged every 10 min. Cells were stimulated with poly(I:C) (20 μg/ml) for up to 60 min (*lower panels*) or left unstimulated (*upper panels*). Fluorescent images of YFP at the indicated time periods are shown. CFP images indicate the expression level of TICAM-1. *C*, Nuclear translocation of IRF-3 induced by poly(I:C) stimulation. HeLa cells were seeded onto cover glass and stimulated with poly(I:C) (40 μg/ml) for up to 120 min. At the indicated periods, cells were fixed, stained with anti-IRF-3 mAb and Alexa Fluor 568-conjugated secondary Ab, and subjected to confocal analyses. Green, IRF-3; blue, nuclei with DAPI; bar, 10 μm.

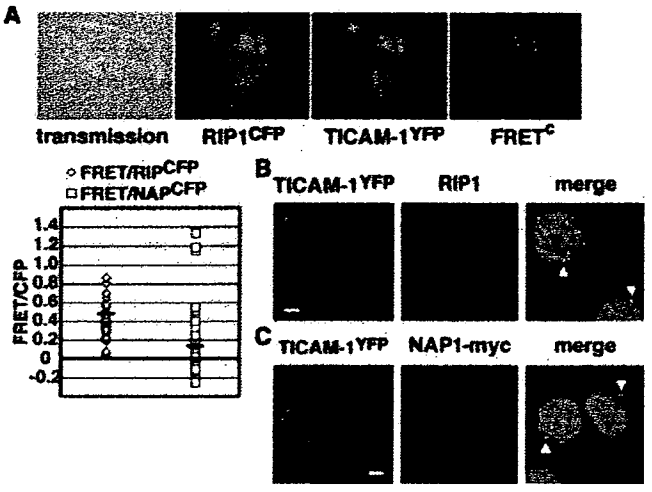

FIGURE 5. RIP1 and NAP1 are recruited to TICAM-1-positive speckles. *A*, Interaction of TICAM-1 with RIP1 or NAP1. HeLa cells coexpressing $RIP1^{CFP}$ or $NAP1^{CFP}$ and $TICAM\text{-}1^{YFP}$ were stimulated with poly(I:C) (20 μg/ml) for 60 min. FRET, YFP, and CFP images were collected by using an inverted fluorescence microscope equipped with a cooled charge-coupled device camera and $FRET^C$ was determined as described in the text. *Upper panels* show FRET images of $RIP1^{CFP}$ and $TICAM\text{-}1^{YFP}$. The *lower graph* shows the normalized FRET values of 60 individual regions of cells calculated by dividing $FRET^C$ for each region by the mean intensity of $RIP1^{CFP}$ or $NAP1^{CFP}$. *B* and *C*, Confocal images of HeLa cells expressing $TICAM\text{-}1^{YFP}$ only (*B*) or $TICAM\text{-}1^{YFP}$ and NAP1-Myc (*C*). Cells were fixed and stained with anti-RIP1 mAb for detecting endogenous RIP1 (*B*) or with anti-Myc mAb (*C*) followed by an Alexa Fluor 568-conjugated secondary Ab. Arrowheads indicate merged speckles. Green, TICAM-1; red, RIP1 or NAP1; blue, nuclei with DAPI; bar, 10 μm.

RIP1 and NAP1 are recruited to TICAM-1-positive speckles

To study the relationship between the translocation of TICAM-1 and its functionality, we next analyzed the subcellular localization of the signaling molecules downstream of TICAM-1. RIP1 is crucial for TICAM-1-mediated NF-κB activation. When RIP1 tagged with YFP ($RIP1^{YFP}$) was coexpressed with a low dose of TICAM-1 tagged with cyan fluorescent protein (CFP; $TICAM\text{-}1^{CFP}$) in HeLa cells, $RIP1^{YFP}$ was uniformly distributed in the cytosol except for constitutive basal RIP1 accumulation (Fig. 4*A*, *upper panels*). Upon poly(I:C) stimulation, $RIP1^{YFP}$ accumulated in the speckle-like structures in a time-dependent manner (Fig. 4*A*, *lower panels*). The speckle formation was detected 30 min after poly(I:C) stimulation and then gradually increased up to 60 min, concomitant with TICAM-1 translocation. In the absence of poly(I:C) stimulation, $RIP1^{YFP}$ remained diffusely in the cytosol (Fig. 4*A*, *upper panels*).

Similar results were obtained with NAP1 tagged with YFP ($NAP1^{YFP}$). NAP1 is located downstream of TICAM-1 and engages in TICAM-1-mediated IRF-3 activation (13). The N-terminal region of TICAM-1 is responsible for the NAP1–TICAM-1 association. When HeLa cells were transfected with $NAP1^{YFP}$ together with $TICAM\text{-}1^{CFP}$ and stimulated with poly(I:C), NAP1 formed the speckle-like structures 30 min after poly(I:C) stimulation, as observed in $RIP1^{YFP}$ localization analyses (Fig. 4*B*). The nuclear translocation of IRF-3 was detected ~60 min after poly(I:C) stimulation, which followed the formation of TICAM-1-positive speckles (Fig. 4*C*).

These results suggest that TICAM-1, once activated by dsRNA-TLR3, interacts with downstream signaling molecules and forms speckle-like structures in the cytosol apart from TLR3. To carry out a precise examination of the molecular interaction between TICAM-1 and RIP1 or NAP1, these molecules tagged with YFP or CFP were coexpressed in HeLa cells and subjected to FRET analysis after poly(I:C) stimulation. As shown in Fig. 5*A*, $FRET^C$ images revealed a strong energy transfer from $RIP1^{CFP}$ to $TICAM\text{-}1^{YFP}$, whereas energy transfer from $NAP1^{CFP}$ to $TICAM\text{-}1^{YFP}$ was relatively weak. These results indicates that RIP1 makes direct contact with TICAM-1 in response to poly(I:C). NAP1 also associates with TICAM-1 in response to poly(I:C), although direct binding was not detected by the yeast two-hybrid technique (data not shown). Thus, TICAM-1 seems to recruit both RIP1 and NAP1 to the putative speckle signalosome. Notably, when TICAM-1 was overexpressed, endogenous RIP1 was highly concentrated in the TICAM-1-positive speckles (Fig. 5*B*). Also, colocalization of TICAM-1 and NAP1 was partly detected in an overexpression study (Fig. 5*C*). At a high TICAM-1 expression level, TICAM-1 might be oligomerized in a TLR3-independent manner and activate downstream signaling molecules to form speckle-like structures. These TICAM-1-positive speckles containing RIP1 and NAP1 barely merged with TLR3 or any organelle markers (data not shown). Because recent reports demonstrated that the internalized dsRNA was trafficked with TLR3 from the endosome to the lysosome in both DCs and epithelial cells (20, 21), the TICAM-1 signaling complex appears to reside in the cytosol distinctly from the dsRNA-TLR3-positive compartments.

Discussion

TLR signaling is mediated by the recruitment of distinct combinations of adaptor molecules to the cytoplasmic TIR domain of each TLR. Distribution and localization of the adaptor molecules are important factors controlling TLR-mediated signaling. TIRAP/Mal was found to be associated with the plasma membrane via a phosphatidylinositol 4,5-biphosphate-binding domain and facilitates MyD88 delivery to activated TLR4 (22). Also, myristoylation of TICAM-2/TRAM targets it to the plasma membrane and the Golgi apparatus, where it colocalizes with TLR4 (23). Thus, the role of these adaptor proteins other than TICAM-1 has been clearly demonstrated; TIRAP/Mal and TICAM-2/TRAM mainly function as bridges between TLR4 and the signaling adaptors, whereas MyD88 restricts its localization by TIRAP to assemble signal molecules around the TLR4 complex (9, 10, 24, 25). In this study we demonstrated that TICAM-1/TRIF delivers a signal in a unique fashion distinct from that of MyD88.

This is the first study to visualize the molecular dynamics of the TICAM-1 pathway that leads to activation of IRF-3 and NF-κB. When TICAM-1 expression is controlled to a low level, TICAM-1 emerges diffusely in the cytosol, whereas overexpressed TICAM-1, which strongly induces IFN-β promoter activation and apoptosis, forms speckles. Neither the diffuse nor speckle form of TICAM-1 colocalizes with endogenous and overexpressed TLR3. Once TLR3 is stimulated with dsRNA in cells with diffuse TICAM-1, TICAM-1 is recruited to the TLR3 inside the cells. Thus, TICAM-1 exists unrelated to TLR3 in resting cells. Whereas dsRNA comes over the cells, TICAM-1 is activated along endosomal TLR3 and then the activated TICAM-1 dissociates from the TLR3 to form a speckle-like structure. The speckle-like structure gathers multiple TICAM-1 molecules according to the confocal feature, suggesting the event of the receptor-induced TICAM-1 oligomerization. This TICAM-1 trip facilitates the focusing of the signaling molecules on the speckle containing TICAM-1 and finally activates NF-κB and IRF-3. In fact, the speckles are comprised of TICAM-1 and the signaling molecules, NAP1 and RIP1. Thus far, however, the intriguing issue as to whether RIP1 and/or NAP1 are recruited to TICAM-1 before or after the dissociation of TICAM-1 from TLR3 remains undetermined. Furthermore, the

mechanism by which TICAM-1 is activated by TLR3 also remains undetermined.

TICAM-1 behaves differently from MyD88, which translocates from the cytosol to the membrane and colocalizes with TLR4 or TLR9 upon ligand stimulation (26). In TLR9-mediated signaling in plasmacytoid DCs, MyD88 forms a stable signaling complex containing IL-1 receptor-associated kinase 4 (IRAK4), TNF receptor-associated factor 6 (TRAF6), and IRF-7 on the cytosolic side of TLR9-resided endosomes (27). MyD88 signaling seems to originate at the TLR-containing complex. By contrast, TICAM-1-mediated signaling events are closely associated with the spatiotemporal mobilization and speckle formation of TICAM-1.

TLR3-TICAM-1 signaling results in various cellular responses, including the production of type I IFN and inflammatory cytokines, DC maturation (28), cross-presentation of exogenous Ags for the proliferation of $CD8^+$ T cells (29, 30), NK cell activation (31, 32), and apoptosis (33). TICAM-1 may act as a platform recruiting signaling molecules for DC output. The signaling components participating in the TICAM-1 mediated type I IFN production have been well characterized. Our current focus is to clarify how these components are orchestrated in undefined molecular cascades. It is becoming clear that the TICAM-1 pathway in myeloid DCs is involved in CTL induction and NK cell activation (29, 32). Through these investigations, the cascades by which the TLR3-TICAM-1 pathway induces cross-presentation and NK activation in myeloid DCs will be defined.

Acknowledgments

We thank Drs. M. Shingai, T. Ebihara, A. Ishii, and A. Matsuo in our laboratory for their critical discussions. We also thank Dr. M. Nakanishi (Nagoya City University, Nagoya, Japan) and Dr. T. Taniguchi (Tokyo University, Tokyo, Japan) for providing plasmids.

Disclosures

The authors have no financial conflict of interest.

References

1. Akira, S., S. Uematsu, and O. Takeuchi. 2006. Pathogen recognition and innate immunity. *Cell* 124: 783–801.
2. Alexopoulou, L., A. C. Holt, R. Medzhitov, and R. A. Flavell. 2001. Recognition of double-stranded RNA and activation of NF-κB by Toll-like receptor 3. *Nature* 413: 732–738.
3. Matsumoto, M., S. Kikkawa, M. Kohase, K. Miyake, and T. Seya. 2002. Establishment of a monoclonal antibody against human Toll-like receptor 3 that blocks double-stranded RNA-mediated signaling. *Biochem. Biophys. Res. Commun.* 293: 1364–1369.
4. Yoneyama, M., M. Kikuchi, T. Natsukawa, N. Shinobu, T. Imaizumi, M. Miyagishi, K. Taira, S. Akira, and T. Fujita. 2004. The RNA helicase RIG-I has an essential function in double-stranded RNA-induced innate antiviral responses. *Nat. Immunol.* 5: 730–737.
5. Oshiumi, H., M. Matsumoto, K. Funami, T. Akazawa, and T. Seya. 2003. TICAM-1, an adaptor molecule that participates in Toll-like receptor 3-mediated interferon-β induction. *Nat. Immunol.* 4: 161–167.
6. Yamamoto, M., S. Sato, H. Hemmi, K. Hoshino, T. Kaisho, H. Sanjo, O. Takeuchi, M. Sugiyama, M. Okabe, K. Takeda, and S. Akira. 2003. Role of adaptor TRIF in the MyD88-independent Toll-like receptor signaling pathway. *Science* 301: 640–643.
7. Matsumoto, M., K. Funami, M. Tanabe, H. Oshiumi, M. Shingai, Y. Seto, A. Yamamoto, and T. Seya. 2003. Subcellular localization of Toll-like receptor 3 in human dendritic cells. *J. Immunol.* 171: 3154–3162.
8. Funami, K., M. Matsumoto, H. Oshiumi, T. Akazawa, A. Yamamoto, and T. Seya. 2004. The cytoplasmic "linker region" in Toll-like receptor 3 controls receptor localization and signaling. *Int. Immunol.* 16: 1143–1154.
9. Oshiumi, H., M. Sasai, K. Shida, T. Fujita, M. Matsumoto, and T. Seya. 2003. TIR-containing adapter molecule (TICAM)-2, a bridging adapter recruiting to Toll-like receptor 4 TICAM-1 that induces interferon-β. *J. Biol. Chem.* 278: 49751–49762.
10. Fitzgerald, K. A., D. C. Rowe, B. J. Barnes, D. R. Caffrey, A. Visintin, E. Latz, B. Monks, P. M. Pitha, and D. T. Golenbock. 2003. LPS-TLR4 signaling to IRF-3/7 and NF-κB involves the Toll adapters TRAM and TRIF. *J. Exp. Med.* 198: 1043–1055.
11. Fitzgerald, K. A., S. M. McWhirter, K. L. Faia, D. C. Rowe, E. Latz, D. T. Golenbock, A. J. Coyle, S. M. Liao, and T. Maniatis. 2003. IKKε and TBK1 are essential components of the IRF3 signaling pathway. *Nat. Immunol.* 4: 491–496.
12. Sharma, S., B. R. tenOever, N. Grandvaux, G. P. Zhou, R. Lin, and J. Hiscott. 2003. Triggering the interferon antiviral response through an IKK-related pathway. *Science* 300: 1148–1151.
13. Sasai, M., H. Oshiumi, M. Matsumoto, N. Inoue, F. Fujita, M. Nakanishi, and T. Seya. 2005. Cutting edge: NF-κB-activating kinase-associated protein 1 participates in TLR3/Toll-IL-1 homology domain-containing adapter molecule-1-mediated IFN regulatory factor 3 activation. *J. Immunol.* 174: 27–30.
14. Meylan, E., K. Burns, K. Hofmann, V. Blancheteau, F. Martinon, M. Kelliher, and J. Tschopp. 2004. RIP1 is an essential mediator of Toll-like receptor 3-induced NF-κ B activation. *Nat. Immunol.* 5: 503–507.
15. Han, K. J., X. Su, L. G. Xu, L. H. Bin, J. Zhang, and H. B. Shu. 2004. Mechanisms of the TRIF-induced interferon-stimulated response element and NF-κB activation and apoptosis pathways. *J. Biol. Chem.* 279: 15652–15661.
16. Kaiser, W. J., and M. K. Offermann. 2005. Apoptosis induced by the Toll-like receptor adaptor TRIF is dependent on its receptor interacting protein homotypic interaction motif. *J. Immunol.* 174: 4942–4952.
17. Sorkin, A., M. McClure, F. Huang, and R. Carter. 2000. Interaction of EGF receptor and grb2 in living cells visualized by fluorescence resonance energy transfer (FRET) microscopy. *Curr. Biol.* 10: 1395–1398.
18. Niimi, K., K. Asano, Y. Shiraishi, T. Nakajima, M. Wakaki, J. Kagyo, T. Takihara, Y. Suzuki, K. Fukunaga, T. Shiomi, et al. 2007. TLR3-mediated synthesis and release of eotaxin-1/CCL11 from human bronchial smooth muscle cells stimulated with double-stranded RNA. *J. Immunol.* 178: 489–495.
19. Yamamoto, M., S. Sato, K. Mori, K. Hoshino, O. Takeuchi, K. Takeda, and S. Akira. 2002. Cutting edge: a novel Toll/IL-1 receptor domain-containing adapter that preferentially activates the IFN-β promoter in the Toll-like receptor signaling. *J. Immunol.* 169: 6668–6672.
20. Lee, H. K., S. Dunzendorfer, K. Soldau, and P. S. Tobias. 2006. Double-stranded RNA-mediated TLR3 activation is enhanced by CD14. *Immunity* 24: 153–163.
21. Johnsen, I. B., T. T. Nguyen, M. Ringdal, A. M. Tryggestad, O. Bakke, E. Lien, T. Espevik, and M. W. Anthonsen. 2006. Toll-like receptor 3 associates with c-Src tyrosine kinase on endosomes to initiate antiviral signaling. *EMBO J.* 25: 3335–3346.
22. Kagan, J. C., and R. Medzhitov. 2006. Phosphoinositide-mediated adaptor recruitment controls Toll-like receptor signaling. *Cell* 125: 943–955.
23. Rowe, D. C., A. F. McGettrick, E. Latz, B. G. Monks, N. J. Gay, M. Yamamoto, S. Akira, L. A. O'Neill, K. A. Fitzgerald, and D. T. Golenbock. 2006. The myristoylation of TRIF-related adaptor molecule is essential for Toll-like receptor 4 signal transduction. *Proc. Natl. Acad. Sci. USA* 103: 6299–6304.
24. Yamamoto, M., S. Sato, H. Hemmi, H. Sanjo, S. Uematsu, T. Kaisho, K. Hoshino, O. Takeuchi, M. Kobayashi, T. Fujita, et al. 2002. Essential role for TIRAP in activation of the signalling cascade shared by TLR2 and TLR4. *Nature* 420: 324–329.
25. Horng, T., G. M. Barton, R. A. Flavell, and R. Medzhitov. 2002. The adaptor molecule TIRAP provides signalling specificity for Toll-like receptors. *Nature* 420: 329–333.
26. Ahmad-Nejad, P., H. Hacker, M. Rutz, S. Bauer, R. M. Vabulas, and H. Wagner. 2002. Bacterial CpG-DNA and lipopolysaccharides activate Toll-like receptors at distinct cellular compartments. *Eur. J. Immunol.* 32: 1958–1968.
27. Honda, K., H. Yanai, T. Mizutani, H. Negishi, N. Shimada, N. Suzuki, Y. Ohba, A. Takaoaka, W. C. Yeh, and T. Taniguchi. 2005. Role of a transductional-transcriptional processor complex involving MyD88 and IRF-7 in Toll-like receptor signaling. *Proc. Natl. Acad. Sci. USA* 101: 15416–15421.
28. Honda, K., S. Sakaguchi, C. Nakajima, A. Watanabe, H. Yanai, M. Matsumoto, T. Ohteki, T. Kaisho, A. Takaoka, S. Akira, et al. 2003. Selective contribution of IFN-α/β signaling to the maturation of dendritic cells induced by double-stranded RNA or viral infection. *Proc. Natl. Acad. Sci. USA* 100: 10872–10877.
29. Schulz, O., S. S. Diebold, M. Chen, T. I. Naslund, M. A. Nolte, L. Alexopoulou, Y. T. Azuma, R. A. Flavell, P. Liljestrom, and C. Reis e Sousa. 2005. Toll-like receptor 3 promotes cross-priming to virus-infected cells. *Nature* 433: 887–892.
30. Salem, M. L., A. N. Kadima, D. J. Cole, and W. E. Gillanders. 2005. Defining the antigen-specific T-cell response to vaccination and poly(I:C)/TLR3 signaling: evidence of enhanced primary and memory CD8 T-cell responses and antitumor immunity. *J. Immunother.* 28: 220–228.
31. Sivori, S., M. Falco, M. Della Chiesa, S. Carlomagno, M. Vitale, L. Moretta, and A. Moretta. 2004. CpG and double-stranded RNA trigger human NK cells by Toll-like receptors: induction of cytokine release and cytotoxicity against tumors and dendritic cells. *Proc. Natl. Acad. Sci. USA* 101: 10116–10121.
32. Akazawa, T., T. Ebihara, M. Okuno, Y. Okuda, M. Shingai, K. Tsujimura, T. Takahashi, M. Ikawa, M. Okabe, N. Inoue, et al. 2007. Antitumor NK activation induced by the TLR3-TICAM-1 (TRIF) pathway in myeloid dendritic cells. *Proc. Natl. Acad. Sci. USA* 104: 252–257.
33. Salaun, B., I. Coste, M. C. Rissoan, S. J. Lebecque, and T. Renno. 2006. TLR3 can directly trigger apoptosis in human cancer cells. *J. Immunol.* 176: 4894–4901.